

AD 731288

SEMI-ANNUAL REPORT

1 Oct 1971

X-RAYS FROM FISSION

Sponsored by

ADVANCED RESEARCH PROJECTS AGENCY

Form Approved Budget Bureau No. 22-R0293

Program Code Number	OF10
ARPA Order Number	1571
Name of Contractor	The University of Texas at Austin
Date of Contract	1 April 1971
Contract Number	N00014-67-A-0126-0012
Amount of Contract	\$133,154
Contract Expiration Date	31 March 1972
Short Title of Work	X-Rays from Fission
Principal Investigators	Dr. Patrick Richard and Dr. C. Fred Moore

Disclaimer: The views and conclusions contained in this document are those of the authors and should not be interpreted as necessarily representing the official policies, either expressed or implied, of the Advanced Research Projects Agency or the U. S. Government.

Reproduced by  
NATIONAL TECHNICAL  
INFORMATION SERVICE  
Springfield, Va. 22151

DISTRIBUTION STATEMENT A  
Approved for public release;  
Distribution Unlimited

D D C  
RECEIVED  
OCT 19 1971  
C  
42

EC

**BEST  
AVAILABLE COPY**

## I. INTRODUCTION

~~This is a report~~ on the activities pursued during the first six months of the second year contract "X-Rays from Fission." The main effort during this part of the contract is to analyze and write-up the research work done using the  $^{252}\text{Cf}$  source. This work involved (X-ray, X-ray) coincidence measurements and (X-ray,  $\gamma$ -ray) coincidence measurements. These experiments have resulted in new findings and have been accepted to be published in The Physical Review, November 1971. The results found in the (X-ray, X-ray) work was in some ways unexpected and we have conjectured that the high correlation of self X-ray coincidences occur due to internal conversion cascading. Furthermore, these internal conversion cascades are highly correlated and are not in agreement with a random or statistical model for the fission process. With this result in mind, one would expect these same measurements to vary with the internal energy of the fissioning nucleus. Thus one should measure X-ray self coincidence as a function of neutron energy for neutron induced fission. Furthermore, this result should vary with respect to the fissionable nucleus. Thus several different targets should be used. If these expectations hold, we believe that we will have a method for determining a quantity, important in determining source characteristics of the nuclide producing fission. At present, our data is the only one available. Thus, we believe this avenue of exploration should be further investigated.

The (X-ray,  $\gamma$ -ray) work has pinned down a large number of  $\gamma$ -ray transitions as to their origin, that is, the specific isotope from

which the transition arises. These  $\gamma$ -ray transitions are the clearest signature by which particular isotopic yields can be identified. Further work will be done since a nearly complete tabulation of gamma-ray energies and their transition properties needs to be tabulated to be confident in making yield determinations.

Since most measurements take approximately one month to run, careful thought needs to be given each experiment before initial data taking is begun. We believe, if no major set-backs develop, that the coming year should produce fruitful results.

II. X-RAY -  $\gamma$ -RAY COINCIDENCE EXPERIMENT:  
MEDIUM ENERGY  $\gamma$ -TRANSITIONS IN  $^{252}\text{Cf}$  FISSION FRAGMENTS

An experiment utilizing X-ray -  $\gamma$ -ray coincidence to distinguish between the  $\gamma$ -rays from the fission fragments of  $^{252}\text{Cf}$  has been performed using a 0.14 cc Ge(Li) detector and a 20 cc Ge(Li) detector.  $\gamma$ -rays in the energy range 150 to 1100 keV have been attributed to pairs of complementary fragments and in several cases to specific isotopes. Agreement with previous data is excellent. Many previously unreported  $\gamma$ -lines have been found. Relative yields within self-gated spectra, as opposed to complementary gated, are being calculated for certain instances where identifications are complete. New information concerning the level schemes of the fission products is forthcoming.

### III. $^{235}\text{U}(n,f)$ $\gamma$ -RAYS

Needed information concerning the fission process is the division of nuclear charge between the primary fission fragments and the associated mass isotopes and excitation energies of the fragment nuclei.

Bent crystal spectroscopy is one method of obtaining part of this information. Walter John and B. G. Saunders, using such a spectrometer at the Livermore Laboratory, determined part of the neutron induced fission yield of  $^{235}\text{U}$  by measuring the energies of many X-rays and  $\gamma$ -rays produced during the fission process. The following light and heavy fission fragments were identified: I, Xe, Cs, Ba, La, Ce, Pr, Nd, Pm, Sm.

It is very interesting to note that the heavy fission fragment spectrum of  $^{252}\text{Cf}$  contains some of the same elements. Therefore it is possible to compare the low energy transitions from the de-excitation of spontaneous fission fragments of  $^{252}\text{Cf}$  observed by F. F. Hopkins et al., in order to make tentative identification of some of the  $\gamma$ -ray lines seen by John and Saunders. Tables I and II contain these identifications for the results of these two experiments.

TABLE I

ISOTOPE	HOPKINS	JOHN
	$E_{\gamma}$ (keV) $\pm$ .15 keV	$E_{\gamma}$ (keV)
$^{116}\text{Rh}$	49.8	49.735 $\pm$ .002
$^{147}\text{La}$	58.1	58.158 $\pm$ .003
$^{146}\text{La}$	64.3	64.375 $\pm$ .007
$^{150}\text{Pr}$	65.5	65.544 $\pm$ .005
$^{108}\text{Tc}$	68.9 (strong)	68.992 $\pm$ .013
$^{141}\text{Cs}$	71.5	71.291 $\pm$ .004
$^{150}\text{Pr}$	74.2	74.259 $\pm$ .007
$^{141}\text{Cs}$	76.5	76.570 $\pm$ .025
$^{140}\text{Cs}$	78.6	78.689 $\pm$ .013
$^{140}\text{Cs}$	80.0	80.095 $\pm$ .019
$^{141}\text{Cs}$	81.7	81.801 $\pm$ .005
$^{146}\text{La}$	82.2	82.515 $\pm$ .010
$^{105}\text{Tc}$	85.6	85.591 $\pm$ .016
$^{136}\text{I}$	87.4	87.323 $\pm$ .010
$^{142}\text{Cs}$	90.3	90.489 $\pm$ .005
$^{101}\text{Y}$	91.0	90.793 $\pm$ .006
$^{142}\text{Cs}$	91.4	91.406 $\pm$ .004
$^{142}\text{Cs}$	96.9	96.851 $\pm$ .008
$^{150}\text{Ce}$	97.7	97.788 $\pm$ .001
$^{101}\text{Y}$	98.2	98.194 $\pm$ .005
$^{141}\text{Ba}$	102.5	102.557 $\pm$ .004
$^{111}\text{Ru}$	103.7	103.497 $\pm$ .008
$^{146}\text{La}$	104.3	104.278 $\pm$ .009
$^{141}\text{Cs}$	106.0	105.887 $\pm$ .027
$^{145}\text{Ba}$	109.8	109.771 $\pm$ .035
$^{109}\text{Tc}$	115.4	115.338 $\pm$ .005
( $^{142}\text{Ba}$ )	117.3	117.313 $\pm$ .004
$^{99}\text{Y}$	122.3	122.248 $\pm$ .006
$^{141}\text{Ba}$	137.9	137.662 $\pm$ .058
$^{104}\text{Mo}$	144.7	144.722 $\pm$ .065
$^{102}\text{Zr}$	151.8	151.772 $\pm$ .020
( $^{148}\text{Ce}$ )	158.7	158.693 $\pm$ .044
$^{106}\text{Mo}$	171.9	171.955 $\pm$ .039

TABLE II

<u>ISOTOPE</u>	<u>HOPKINS</u> <u>E<sub>γ</sub> (keV)</u>	<u>JOHN</u> <u>E<sub>γ</sub> (keV)</u>
I or Rh	65.8, 65.5	65.544±.005
	82.5, 82.3	82.515±.010
	212.7	212.617±.019
Xe or Ru	107.7, 102.6	102.645±.035
Cs or Tc	54.5	54.595±.004
	64.4 64.1	64.375±.007
Ba or Mo	50.1	50.127±.003
	58.1	58.158±.003
	64.3	64.375±.007
	65.9, 66.4	65.923±.004
	98.2	98.194±.005
La or Nb	46.9, 46.4	46.575±.003
		46.670±.006
	56.2, 56.0	56.076±.005
	66.2, 65.9	65.923±.004
	67.1, 66.9	67.121±.005
	73.6	73.541±.003
	77.6, 77.6	77.578±.011
97.0, 96.9	96.851±.008	
Ce or Zr	52.2	52.175±.005
	55.0, 54.7	54.695±.005
		55.009±.004
	64.3, 64.3	64.375±.007
	87.3	87.323±.010
	117.695±.012	
Pr or Y	117.8, 117.6	117.695±.012
	68.9	68.992±.013
	76.6	76.570±.025
	79.9	79.986±.010
	87.6	87.618±.016
	103.497±.008	
	103.4	103.497±.008

#### IV. FISSION FRAGMENT TIME-OF-FLIGHT

Initial attempts to use a quadrupole to focus  $^{252}\text{Cf}$  fission fragments onto a detector located about 8 meters from the fissioning source have not, as yet, met with overwhelming success.

A full scale experiment has not yet been undertaken, however, because an adequate source is not yet available. When we placed the present source inside a chamber, the chamber and silicon detector became contaminated. Another such attempt is not planned until we secure a covered source. Upon inquiry, Mr. E. H. Kobish of the Oak Ridge National Laboratory, advised us that a source covered with as little as  $25 \mu\text{g}/\text{cm}^2$  of carbon transmitted no significant amount of californium, and that for this film density, the energy loss observed for the medium light and medium heavy fragments was  $\sim 1.4$  and  $1.0$  MeV respectively.

We are presently considering construction of an apparatus such as was described by Oakey & MacFarlane (Nucl. Instru. & Meth., 49 (1967) 220), wherein a wire stretched down the center of a beam tube and maintained a high voltage allowed electrostatic focusing of charged particles. (Another paper by Hooverman, Jour. Appl. Phys. 34 #12, 3505, discussed the trajectories of charged particles about such a wire). This particular apparatus would probably be used in conjunction with a quadrupole to focus the fragments.

The greatest single problem in this experiment is that of the extremely low count rate. After counting for 8 hours, only one count could be attributed to a fission fragment. Limitations on the thickness of a source as determined by the range of the fragments in  $^{252}\text{Cf}$  indicate that even the strongest possible source will have an extremely low count rate.

## V. EXPLANATION OF THE CNS CONTINUOUS THROUGHPUT DISK HISTOGRAM SYSTEM:

### Histogram generation:

The data-taking multiparameter program outputs 18-bit numbers into core memory buffers for transfer in 2048-word blocks onto 64K disk data buffers. These numbers are addresses to be incremented on the histogram disk. Both the core buffers and the disk buffers are double buffers; that is, one half of the total space is being processed while the other half is being filled. This means input can be continuous, without pause for updating the disks or waiting for completion of core/disk data transfers.

When one of the two disk data buffer areas is filled, the program starts filling the other one and begins processing of the full one. The aim of this processing is to have each word in the disk data buffer being processed cause an increment of the address on the histogram disk named by that word. The processing proceeds as follows:

(a) The first sector of the histogram disk is read into a section of core memory reserved for this purpose. (The size of this section of memory can be 4K, 8K, or 16K)

(b) A command is given to a special interface to read a part of the disk data buffer. The interface compares the high order bits of each word read from the disk with those high order bits common to all the histogram addresses of the sector now in core. (Thus if a 4K core buffer is used, a copy of disk addresses 450000-457777 might be in core at one time; it is the high order six bits [45 in this example] that would then be compared with the high order six bits of the words read from the disk data buffer.)

If the compared bits are different, then the histogram sector addressed by the word is not in memory at that time, and the work is ignored. [Note that this takes no computer time at all.] If the compared bits are the same, then the word refers to the histogram sector then in memory. The low order (uncompared) bits are then used to increment the correct word of the histogram sector via an automatic increment facility. This steals a little time ( $\sim 2\mu\text{sec}$ ) from the program, but does not require program attention. (Prior to input to the increment channel, the low-order bits are suitably relocated by a hardware add-on of the starting address of the memory area reserved for histogram sectors).

This process is continued until the full disk data buffer list has been compared to the histogram sector in core. This sector then has been updated. It is unnecessary to delete the words used to update the sector from the disk data buffer list, since these words will fail all subsequent comparisons because this sector will not be in core again during this processing cycle.

(c) The updated sector is written back in its place on the disk, overwriting the old version. If this was not the last sector, the next sector is read in and (b) is repeated.

After the last sector of the histogram is updated, the whole process is repeated on the portion of the other disk data buffer which has been filled during the previous cycle.

## MATHEMATICAL ANALYSIS OF TIMING AND SPACE ALLOCATION:

### (a) Symbolism

I = size of each of the two data input buffers.

M = size of the memory section reserved for histogram sector processing.

C = size of area processed by one compare command

D = size of each disk data buffer

H = size of histogram disk area

T<sub>1</sub> = time to put a word into an input buffer

T<sub>2</sub> = time to initiate core/disk transfer

T<sub>3</sub> = hardware time/word for core/disk transfers

T<sub>4</sub> = hardware time/word for increment breaks

Then the total time to process a full disk data buffer is:

$$T_T = D \cdot T_1 + (D/I) \cdot T_2 + D \cdot T_4 + (H/M) (T_2 \cdot [2 + D/C]) + H \cdot 2 \cdot T_3 + D \cdot T_3$$

and the time/word is:

$$T = T_1 + T_2/I + T_4 + 2 \cdot T_2 \cdot H / (M \cdot D) + T_2 \cdot H / (C \cdot M) + (H/D) \cdot 2 \cdot T_3 + T_3$$

### TIME FOR TYPICAL HARDWARE AND PROGRAMMING VALUES IN SLOWEST CONFIGURATION

I = 2048 words

M = 4096 words

C = 2048 words

D = 65,536 words [1/4 DEC R509 disk]

H = 262,144 words [1 disk]

T1 = 4 microseconds

T2 = 50 microseconds

T3 = 5 microseconds

T4 = 3 microseconds

Then  $T = 4 + 1/400 + 3 + 1/10 + 1/2 + 40 + 5$

<54 microseconds/word

The greatest contribution is proportional to H/D; all other significant contributions are not affected by the choice of the various parameters. Reducing the histogram size would decrease time/word proportionally. Use of a full disk for each data buffer would reduce the time/word to 24 microseconds for 256K histograms.

The maximum data rate is not limited by the time/word, however, but rather by the speed of rotation of the disks. If the time of rotation per disk word is R microseconds, then the time required for a full processing cycle:

$$T_p = R(D + (H/M(D+4M)))$$

For R equals 15 microseconds and other parameters as stated above, this total time is 85 seconds. For the 64K increments involved this gives a increment rate of about 765 increments/second. This rate is almost proportional to M/H and can thus be increased either by increasing the core buffer or using only a portion of the histogram disk. With a 16K buffer, the rate for a full disk is 1860 increments/second.

An important thing to note is that only about 3.5 seconds of processor time is required for each 85-second cycle. This leaves the program free 92% of the time for list analysis, display, and command execution. Usually a multi-parameter analysis complex enough to use 256K histogram space generates fewer than 1000 increments/second. Thus the disk increment system is usually not the limiting part of the analysis procedure.

VI. PERSONNEL

1 April 1971 to 30 September 1971

(a) Nuclear Scientists

Patrick Richard, Associate Professor	1 month
C. Fred Moore, Professor	1 month
Gerald Hoffmann, Research Scientist IV	2 days
Gary Phillips, Research Scientist IV*	5 months

(b) Pre-Doctoral Appointments (graduate students)

Forrest Hopkins, Research Assistant III	6 months
John R. White, Research Assistant II	6 months
Dee McCrary, Research Assistant II	2 months
Rolf-Gerald Abitz, Research Assistant I	2 months
Mike Picone, Research Fellow*	6 months
Bill Hodge, Research Assistant II	5 months
Mike Senglaub, Research Assistant II	5 months
Joseph Gibbs, Research Assistant II	3 months
Rodrigue St-Laurent, Research Fellow*	6 months

(c) Engineering/Technical Staff

Mary George, Administrative Clerk*	6 months
Kenric Speed, Laboratory Assistant II	6 months
John P. Coose, Technical Assistant III	6 months
Hunter Ellinger, Programmer I*	6 months
Alvin L. Mitchell, Research Engineer III*	6 months

(d) Laboratory Staff (undergraduate students)

Jerry Baker, Laboratory Assistant III	3 months
Jeffery Fitch, Laboratory Assistant III	6 months
Terry Lindsey, Laboratory Assistant IV	5 months
Nat Smith, Laboratory Assistant I	3 months
Roger Jordon, Laboratory Assistant II	4 days
Tom Loyd, Laboratory Assistant II	4 days

\* At no pay

## APPENDIX I

### INTERNAL CONVERSION CASCADES IN FISSION PRODUCTS\*

Rodrigue St-Laurent<sup>+</sup>, Gary W. Phillips

Patrick Richard and C. Fred Moore

Physics Department, Center for Nuclear Studies

University of Texas, Austin, Texas 78712

#### ABSTRACT

A two parameter coincident (X-ray, X-ray) measurement was made using a Si(Li) X-ray detector and a Ge(Li) X-ray detector to study the X-ray production in the  $^{252}\text{Cf}$  fission process. K X-ray peaks from adjacent Z fission products are well resolved in both detectors. The measurement yields the result that there is a large number of coincident events with X-rays from the same Z element as well as with X-rays from the complementary fission product, (e.g. Cs K X-rays are in coincidence with both the complementary Tc K X-rays and the Cs K X-rays). The various possibilities one may consider are: (1) K X-ray production by the primary fission process followed by internal conversion, (2) multiple K X-ray production in the stopping process of the fission products, (3) K shell ionization resulting from  $\beta$ -decay of the fission fragments followed by internal conversion in the same fragment, and (4) multiple internal conversion processes from cascading transitions. Each of these four possible causes for self coincident X-ray production is explored.

FISSION  $^{252}\text{Cf}$  - fission, X-ray: X-ray coincidence, internal conversion cascades deduced from data. K X-ray range 10 to 50 keV.

## I. INTRODUCTION

This paper reports the observation of internal conversion cascades in nuclei formed by the fission of  $^{252}\text{Cf}$ . The measurement involves the detection of the X-rays following internal conversion transitions. The development in recent years of high efficiency, high resolution solid state detectors to measure the X-rays produced in a fission event in coincidence with other processes has renewed interest in the study of fission yields. The fission process produces highly excited fragments with unstable nuclei having very short half-lives. Their electromagnetic radiations as well as their beta-decay and their internal conversion electrons form complicated spectra that can be analyzed most efficiently by coincidence techniques.<sup>1,2,3</sup> These have been used to determine the charge, mass and energy of the fragments in order to identify the isotopes with short lives that are produced during the fission.<sup>4,5,6,7</sup>

The most rudimentary X-ray coincidence measurement to make, but one which has not been reported previously,<sup>8</sup> is that of (X-ray, X-ray). The present measurement gives the result that not only do the complementary fission products produce coincident K X-rays, but also coincident K X-rays from the same Z element are produced with comparable and more often much greater magnitude. This obviously can happen only by some means of multiple successive K shell ionizations in the same element, since double K shell ionization will shift the X-ray energies appreciably for the first of the two K X-ray transitions.

## II. EXPERIMENTAL PROCEDURE

### A. Source and Detectors

A small  $^{252}\text{Cf}$  source (approximately 550 fissions/sec) was sandwiched between two pieces of cellophane tape ( $\text{C}_{10}\text{H}_8\text{O}_4$ ) and placed between the faces of two semi-conductor detectors with 1.0 mm and 5.0 mm Beryllium windows. The cellophane tape stopped the fission fragments and as far as can be determined prevented Doppler distortions in the X-ray spectra while obtaining the maximum coincidence rate.

The X-rays were detected by high resolution Ge(Li) and Si(Li) detectors. The Ge(Li) detector had an approximate active volume of 0.14 cc and the Si(Li) detector approximately 0.03 cc. A resolution of about 325 eV full width at half maximum at 18 keV was obtained with both detectors.

The efficiency, in the range of operation from 10 keV to 40 keV was 100% for the Ge(Li) detector and from 100% to 28% for the Si(Li) detector. Corrections due to counter efficiency have been made with respect to measurements dependent on the Si(Li) detector. The solid angle of each of the two detectors was about 0.5 sr. This experiment was repeated with two 100% Ge(Li) detectors and the results agree within statistics.

### B. Coincidence System

Pulses generated in the Si(Li) and the Ge(Li) detectors by the X-rays were amplified and passed through constant fraction timing discriminators as shown in Fig. 1. The timing signals from the fast discriminators were sent to a time-to-pulse-height converter (TPHC). It

was required that the X-rays be detected within the time interval of 50 nanoseconds in order to generate a gating signal through a signal-channel analyzer (SCA). The linear X-ray pulses from both detectors and the output of SCA were routed to three 1024 channel analog-to-digital converters (ADC). A two-parameter analysis was then performed on line via a PDP-7 and PDP-15 computer system. The gated linear signals from the Ge(Li) detector were sorted and stored in 1024 channel spectra according to windows set in the computer on the X-ray peaks in the gated spectrum from the Si(Li) detector.

#### C. Calibration

The two X-ray spectra were calibrated with  $^{55}\text{Fe}$  and  $^{133}\text{Ba}$  sources and by observing the position of the known peaks of the X-rays of the light and heavy fission fragments. The energies of the other peaks were determined by a least squares' fit to a third order polynomial function. The gains of the amplifiers were checked at every 10-hour run by noting the position of the prominent peaks of each spectrum. The set-up was stable enough that no gain adjustments were required.

#### D. Windows

When the peaks in the X-ray spectrum of the Si(Li) detector contained a sufficient number of counts, gates were set on the  $K_{\alpha_{1,2}}$  X-ray peaks of 14 fission fragments (as indicated in Fig. 2) by the channel location in which these X-ray peaks were stored in the spectrum. After a 107-hour run the 7 pairs of spectra: Y-Pr, Zr-Ce, Nb-La, Mo-Ba,

Tc-Cs, Ru-Xe and Rh-I were graphed and compared with the total X-ray coincident spectrum obtained from the Ge(Li) detector. Figs. 3a-g show these spectra.

### III. RESULTS

Numerical results of this experiment are tabulated in Table I. The intensities are given relative to Tc and corrected for the efficiency of the Si(Li) detector which varies from 100% for Y to 28% for Pr. The intensity of the  $K_{\alpha}$  X-ray from the light fragment is usually about the same whether the window is on the heavy or on the light fragment X-ray. The inverse is usually not so. The intensity of the heavy fragment X-ray is usually much greater in self coincidence. Exceptions to this are Tc-Cs and Ru-Xe pairs. In the fourth column of Table I are listed the intensity ratios of the  $K_{\alpha}$  X-ray lines of each of the fission products with the  $K_{\alpha}$  X-ray of the complementary fission product. In most cases the ratio of self coincidence to complementary coincidence is greater than one for the heavy fragments and less than one for the light fragments; the only exceptions are Tc and Ru with the ratios greater than one. Fig. 4 shows a bar graph of the results tabulated in Table I.

The coincidence X-ray spectra given in Figs 3a-g show the total X-ray spectrum compared with the coincidence spectra for the complementary pairs. The prominent peaks are the characteristic  $K_{\alpha}$  and  $K_{\beta}$  lines. The self coincidence is usually more prolific than the complementary X-ray production. There are several spectra where prominent peaks

apparently due to low energy gamma rays are observed, e.g. Y (Fig. 3a) where a peak appears at about the Ru  $K_{\alpha}$  energy, but no Ru  $K_{\beta}$  is seen.

The remainder of the discussion will be devoted to explanations of processes which may give rise to multiple X-ray yield from a single fragment. The various possibilities one may consider are: (1) K X-ray production by the primary fission process followed by internal conversion, (2) multiple K X-ray production in the stopping process of the fission products, (3) K shell ionization resulting from  $\beta$ -decay of the fission fragments followed by internal conversion in the same fragment, and (4) multiple internal conversion processes from cascading transitions. These will be discussed below.

(1) The presently accepted source of K X-ray production in fission processes is the X-ray following an internal conversion electron transition in the nuclear de-excitation of a fission product.<sup>4,5</sup> The primary fission process itself is thought to be adiabatic in the rearrangement in the K shell electron configurations for the fission products. This is believable since the velocity of the K shell electron is much faster than the velocity of the fission product itself. Thus the two K electrons would fill their respective shells in each of the fission products as they emerge from the electron cloud of the californium atom, and consequently no primary K X-ray would be produced. If this were a source of the X-ray production, the X-rays would be Doppler shifted and would not appear as a single narrow line in our spectra. The fission product will stop in  $10^{-12}$  seconds, and the lifetimes of the K X-ray transitions are of the order

of  $10^{-16}$  seconds.

(2) In the present experiment the fission fragments were stopped in  $C_{10}H_8O_4$  (cellophane tape) which was in contact with the source. The stopping process of the fission products in the tape is not a likely source of K X-ray production. From cross section calculations using the tables of Khandelwal et al.<sup>9</sup> for the case of the most probable mass and energy of technetium (104 u, 100 MeV), it was found that the number of K X-rays expected from these fragments when they are stopped was about  $10^{-6}$  X-rays per fragment or 70 K X-rays after a 107-hour run, which is negligible.

(3) A third possible explanation for double K X-ray production leading to X-ray self coincidence is K shell ionization produced by nuclear beta-decay of the fission fragment followed by internal conversion. The probability that beta-decay causes K shell ionization has been studied both theoretically<sup>10,11,12</sup> and experimentally.<sup>13,14</sup> An accurate estimate of this probability can be made using Migdal's result which is  $P_k = 0.64/Z^2$ . The  $1/Z^2$  dependence favors K ionization for the light fragments, thus an optimistic estimate of the effect can be made by considering the case of a Zr fission fragment. For this case  $P_k$  is  $4 \times 10^{-4}$ . With such a small probability it seems unlikely that this can be the source of K X-ray self coincidence.

(4) Multiple internal conversion involves two or more internal conversions in cascade. In the literature there are a few cases where internal conversion cascades are likely, e.g., the decay of  $^{117}\text{Sn}$  (317 keV, 158 keV).<sup>15</sup> For the 158 keV M1 transition, the K shell internal conversion

coefficient  $\alpha_K$  was measured to be 0.137 which compared well with calculated values. The 317 keV M4 transition feeding the 158 keV level has a 14 day half-life and  $e/\gamma$  is listed as being very large.<sup>16</sup> Thus for low energies, internal conversion cascades can compete favorably with gamma decay cascades even for multipole orders as low as M1.

The following considerations show that the latter process<sup>4</sup> can explain the data even though it may intuitively seem unlikely:

(a) The experiment discussed above and tabulated values<sup>17</sup> for  $\alpha_K$  show that internal conversion is probable for low-energy transitions in the mass range of the fission fragments.

(b) Recent experiments show a large number of low-energy gamma rays in coincidence with K X-rays from <sup>252</sup>Cf fission.<sup>2,7</sup>

(c) The odd Z elements have the largest number of low-energy transitions, but in general the multipolarities are not known so the internal conversion probabilities cannot be given with certainty. One case where two gamma rays with known multipolarities are known to be in cascade<sup>18,19</sup> is for the 97 keV  $2^+ \rightarrow 0^+$  and 209 keV  $4^+ \rightarrow 2^+$  transitions in <sup>150</sup>Ce. The respective E2 K shell conversion probabilities  $P_K = \frac{\alpha_K}{1+\alpha_K}$ , neglecting L shell conversion, are 0.58 and 0.11.<sup>17</sup>

(d) The results shown in Table I show large variations with Z and are without any noticeable systematic trend. Thus a nuclear process, internal conversion, is more likely. An atomic process would be expected to show a smooth dependence with Z.

(e) The predominance of self coincidence seems to indicate that

the majority of the observed X-rays occur following isomeric transitions or after  $\beta$ -decay so that they are not in prompt coincidence with X-rays from the complementary fragment.

#### IV. CORRELATION EFFECTS

Prompt fission X-ray coincidence yields for random population of nuclear levels in the fission products will be proportional to (total X-ray yield for heavy fragment) times (total X-ray yield for complementary light fragment). This result dictates that the ratio  $(K_L/K_H)_{\text{complement}} = 1.0$ , since complementary X-ray coincidence production can arise only from prompt processes. This result is approximately born out, as seen in Table I, for the ratios Y/Pr, Mo/Ba, Ru/Xe, and Rh/I. However, the ratios Zr/Ce, Nb/La, and Tc/Cs are far from unity. The last column in Table I shows the result one should obtain for random X-ray events using the yields obtained by Watson et al.<sup>2</sup> The last column shows little agreement with the relative intensities in column 3. This is evidence that nuclear level population in fission fragments is strongly correlated. That is, if one fragment de-excites via internal conversion, the probability of the complementary fragment being in a state which also decays by internal conversion is not random. This is consistent with conservation laws, but has never been shown.

#### V. CONCLUSION

The results of this work leave many questions which can be answered only by further experimentation. Certainly more detailed knowledge

of the structure of these nuclei is needed.

Nuclear shell effects are evident in the almost complete lack of X-rays from Te (Z=52) and the low intensity of X-rays from Xe (Z=54) which have proton numbers near the closed shell at 50. Those isotopes of Te and Xe observed in  $^{252}\text{Cf}$  binary fission also have neutron numbers near the N=82 closed shell.<sup>18</sup> Thus their low-lying levels are more widely spaced resulting in higher energy transitions and correspondingly much lower probabilities for internal conversion.

It seems that multiple internal conversion is the process dominating the observation of K X-rays in self coincidence. Electron-electron coincidence experiments involving internal conversion electrons would help confirm this hypothesis.

## REFERENCES

\*This research was supported in part by the Advanced Research Projects Agency of the Department of Defense and was monitored by the Office of Naval Research under Contract No. N00014-67-A-0126-0012.

+Fellow, Université du Québec à Chicoutimi.

1. R. L. Watson, Phys. Rev. 179 (1969) 1109.
2. R. L. Watson, H. R. Bowman and S. G. Thompson, Phys. Rev. 162 (1967) 1169.
3. T. Alvager, R. A. Naumann, R. F. Petry, G. Sidenius and T. Darrah Thomas, Phys. Rev. 167 (1968) 1105.
4. L. E. Glendenin and J. P. Unik, Phys. Rev. 140 (1965) B1301.
5. J. B. Wilhelmy, Ph.D. dissertation, University of California, Berkeley, (1969).
6. D. R. Rueggeger, Jr., and R. Roy, Phys. Rev. C1 (1969) 631.
7. F. F. Hopkins, G. W. Phillips, J. R. White, C. F. Moore and Patrick Richard, to be published.
8. Work on X-ray, X-ray coincidences is concurrently being carried at Trombay, Bombay, India, (S. S. Kapoor, private communication).
9. G. S. Khandelwal, B. H. Choi, and E. Merzbacher, Atomic Data 1, (1969) 103.
10. A. Migdal, J. Phys. (USSR) 4 (1941) 449.
11. E. L. Feinberg, J. Phys. 4 (1941) 424.
12. J. S. Levinger, Phys. Rev. 90 (1953) 11.

13. T. E. Novey, Phys. Rev. 86 (1952) 619.
14. Yasuhito Isozumi and Sakae Shimizu, Phys. Rev., to be published.
15. J. P. Bocquet, Y. Y. Chu, G. T. Emery, and M. L. Periman, Phys. Rev. 167 (1968) 1117.
16. C. M. Lederer, J. M. Hollander, I. Perlman, Table of Isotopes, Sixth Ed., John Wiley & Sons, (1968).
17. R. S. Hager and E. C. Seltzer, Nuclear Data 4A (1968) 1.
18. J. B. Wilhelmy, S. G. Thompson, R. C. Jared, and E. Cheifetz, Phys. Rev. Lettrs. 25 (1970) 1122.
19. E. Cheifetz, R. C. Jared, S. G. Thompson and J. B. Wilhelmy, Phys. Rev. Lettrs. 25 (1970) 38.

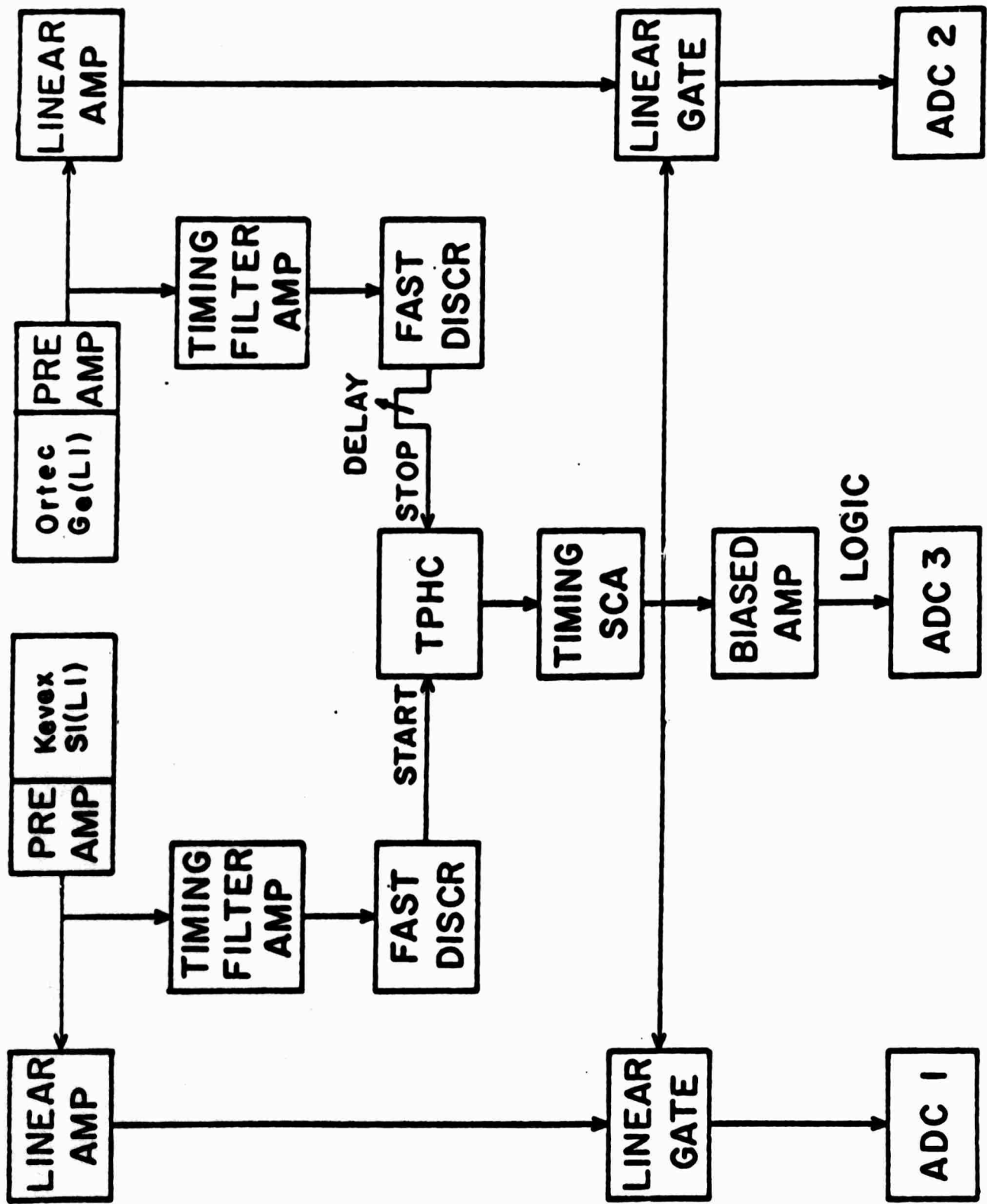
Table I:  $^{252}\text{Cf}$  Fission X-ray Coincidence Normalized Intensities and Intensity Ratios with  $I_{\text{Tc}} = 1$ , for Self Coincidence.

Window Set On	Relative Intensities		$\frac{(K_{\alpha}^{\text{self}})}{(K_{\alpha}^{\text{comp}})}$	$P^{(a)}$
	$(K_{\alpha}^{\text{self}})$	$(K_{\alpha}^{\text{complement}})$		
Y	0.11±.01	0.13±.01	0.86±0.09	0.02±0.004
Pr	0.97±.06	0.10±.01	9.7 ±1.2	
Zr	0.04±.01	0.17±.01	0.24±0.03	0.06±0.007
Ce	0.62±.04	0.06±.01	11.0 ±1.7	
Nb	0.10±.01	0.33±.02	0.31±0.02	0.10±0.013
La	1.55±.03	0.11±.01	14.0 ±1.4	
Mo	0.08±.01	0.18±.01	0.45±0.39	0.11±0.013
Ba	0.16±.02	0.13±.02	1.2 ±0.16	
Tc	1.00±.04	0.60±.03	1.7 ±0.08	0.38±0.046
Cs	1.68±.07	0.39±.03	4.3 ±0.23	
Ru	0.37±.02	0.06±.01	5.8 ±0.55	0.06±0.008
Xe	0.10±.01	0.06±.01	1.7 ±0.25	
Rh	0.13±.01	0.15±.01	0.85±0.07	0.06±0.008
I	0.16±.06	0.10±.01	11.6 ±1.2	

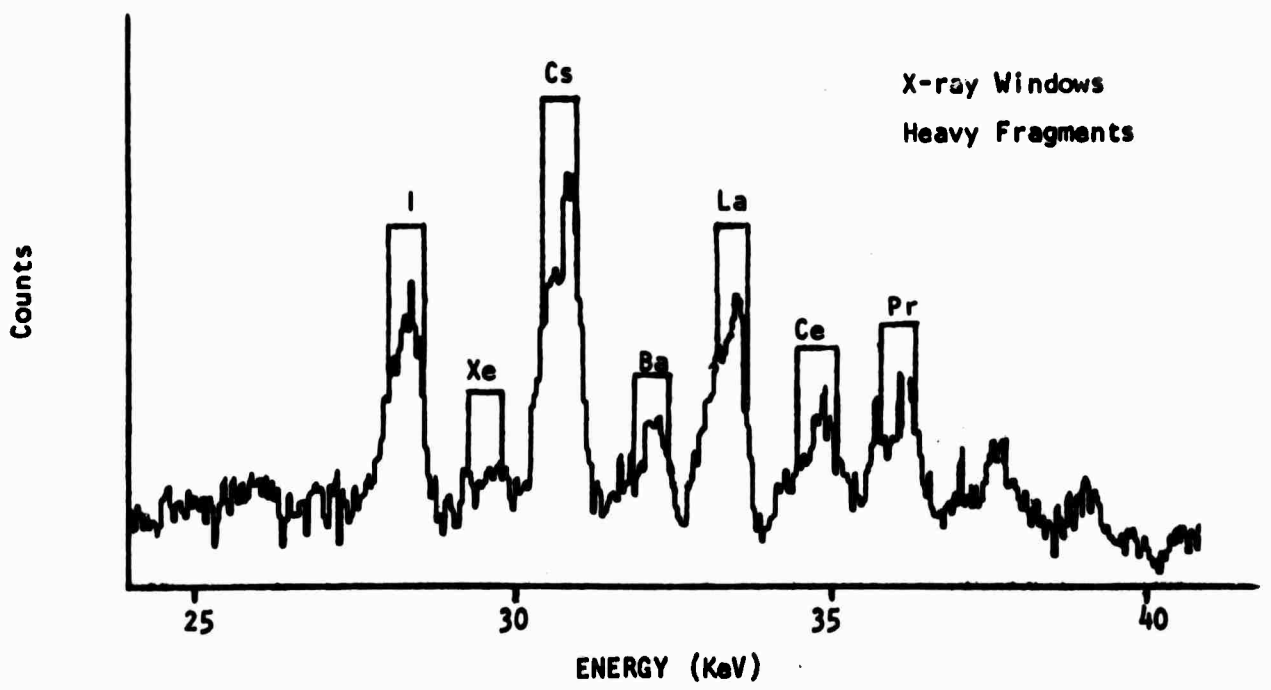
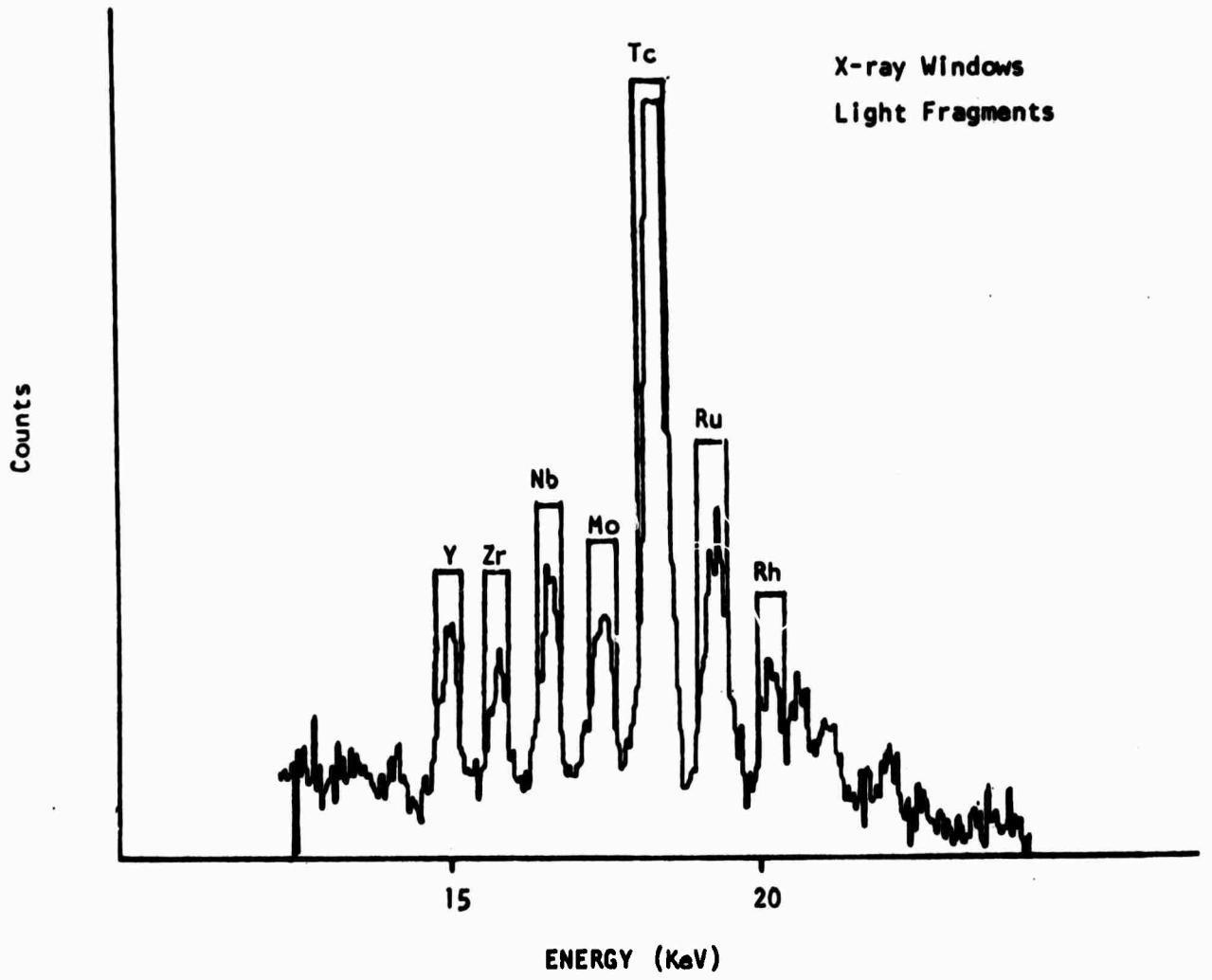
(a)  $P$  is the product of  $K$  X-ray yields of complementary fragments from primary  $^{252}\text{Cf}$  fission products normalized to the Ru/Xe  $K_{\alpha}$  complement from column 3. The yields were taken from ref. 2, Table I.

## FIGURE CAPTIONS

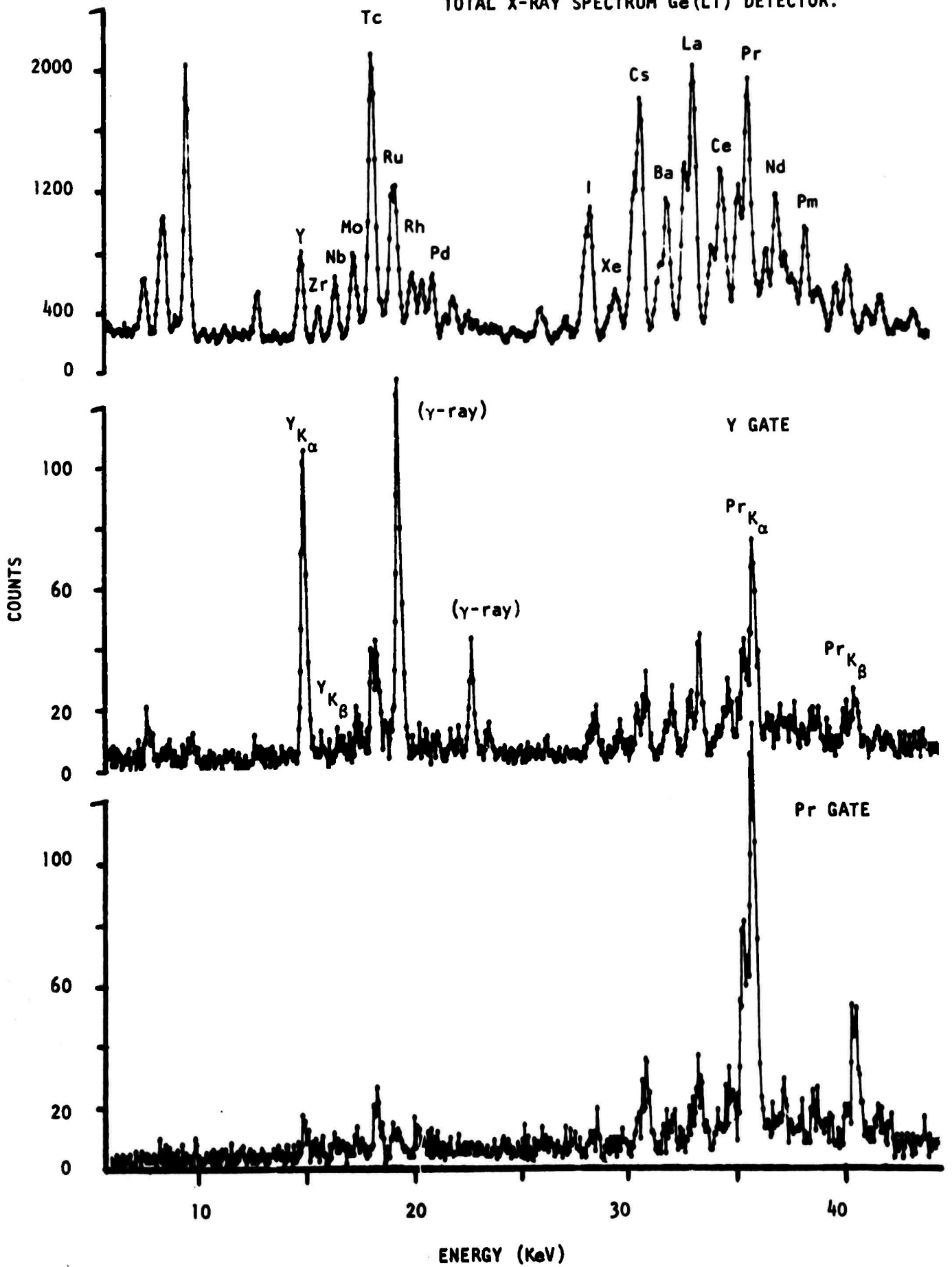
- Fig. 1 Schematic diagram of electronics.
- Fig. 2 Windows set on light and heavy fragments X-rays.
- Fig. 3 X-ray spectra obtained in coincidence with windows set on
- (a) Yttrium Praseodymium, compared with the total X-ray spectrum;
  - (b) Zirconium and Cerium, compared with the total X-ray spectrum;
  - (c) Niobium and Lanthanum, compared with the total X-ray spectrum;
  - (d) Molybdenum and Barium, compared with the total X-ray spectrum;
  - (e) Cesium and Technetium, compared with the total X-ray spectrum;
  - (f) Ruthenium and Xenon, compared with the total X-ray spectrum;
  - (g) Rhodium and Iodine, compared with the total X-ray spectrum.
- Fig. 4 Results tabulated in Table I are shown as a bar graph. X-ray production from each fission product is compared to its complement.



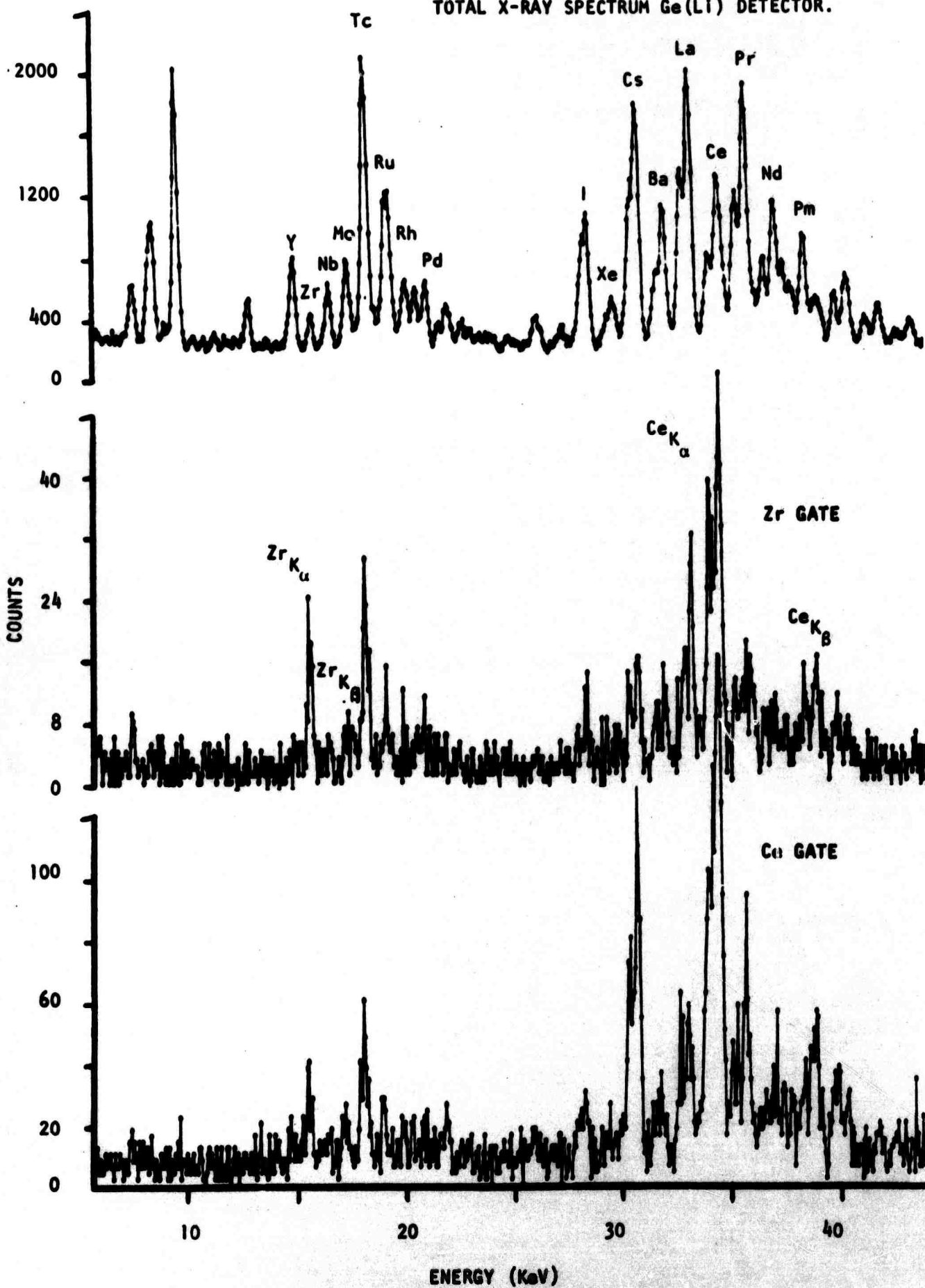
CIRCUITRY USED IN COINCIDENCE EXPERIMENT.



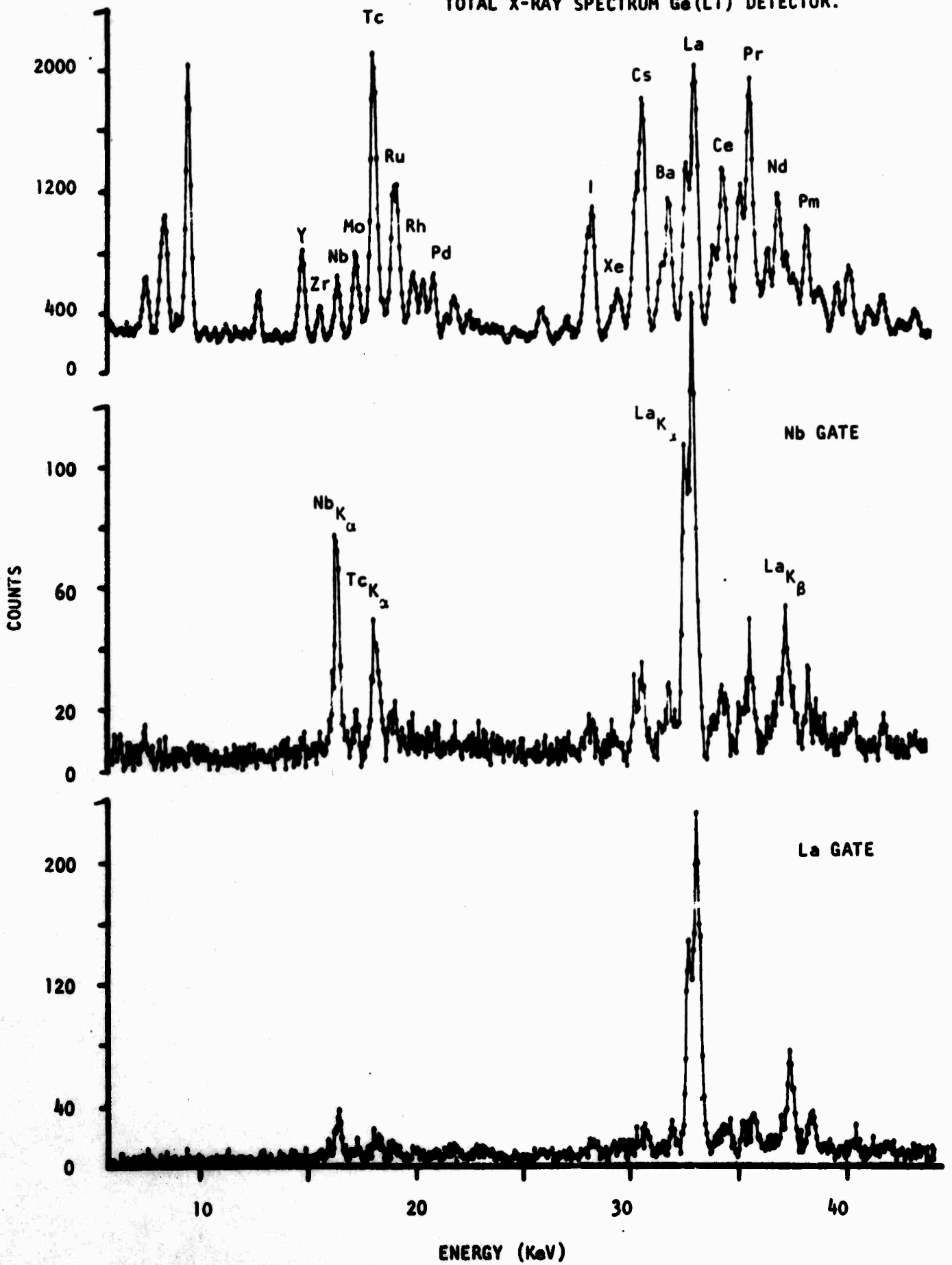
TOTAL X-RAY SPECTRUM Ge(Li) DETECTOR.



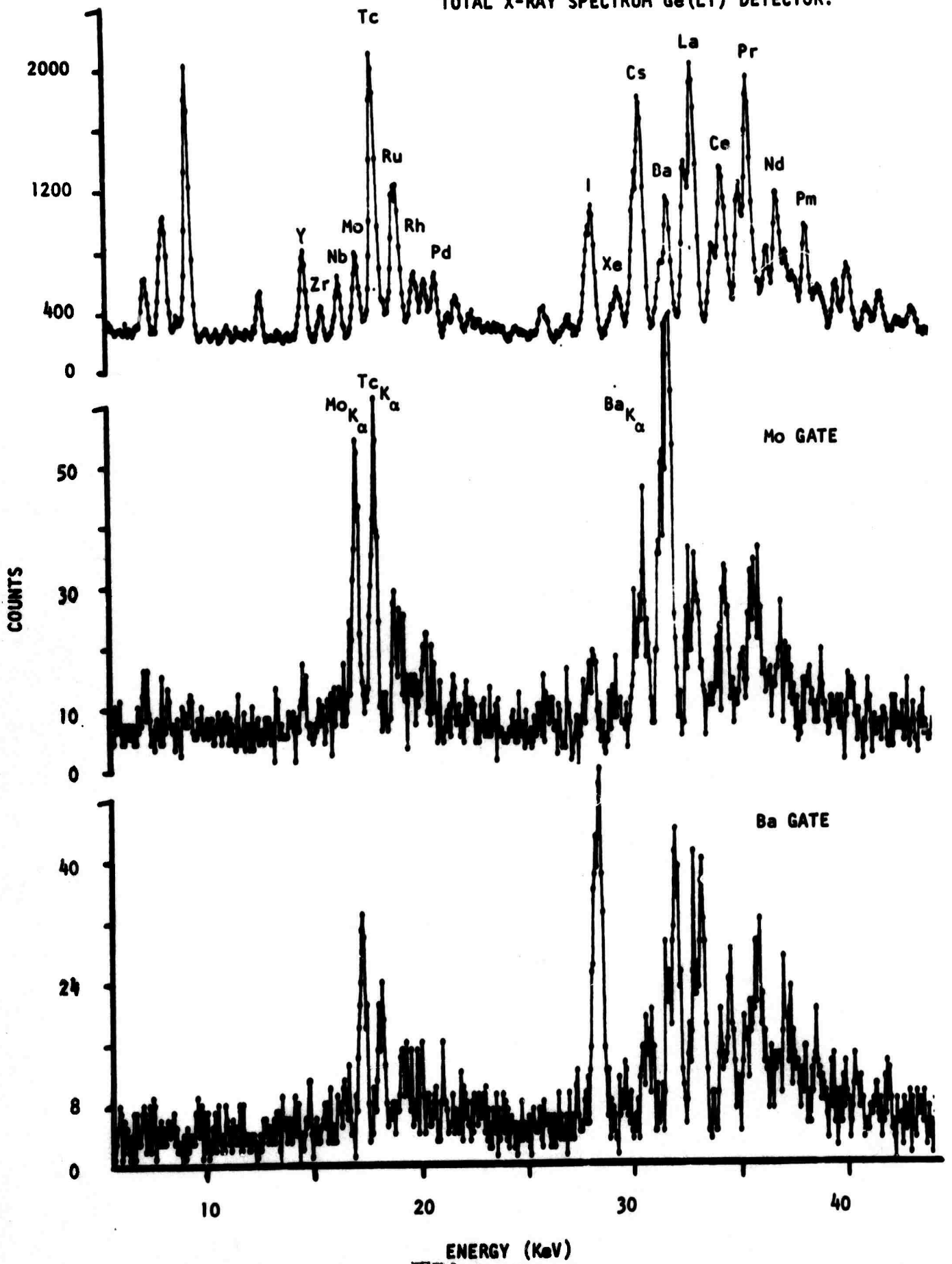
TOTAL X-RAY SPECTRUM Ge(LI) DETECTOR.



TOTAL X-RAY SPECTRUM Ge(Li) DETECTOR.



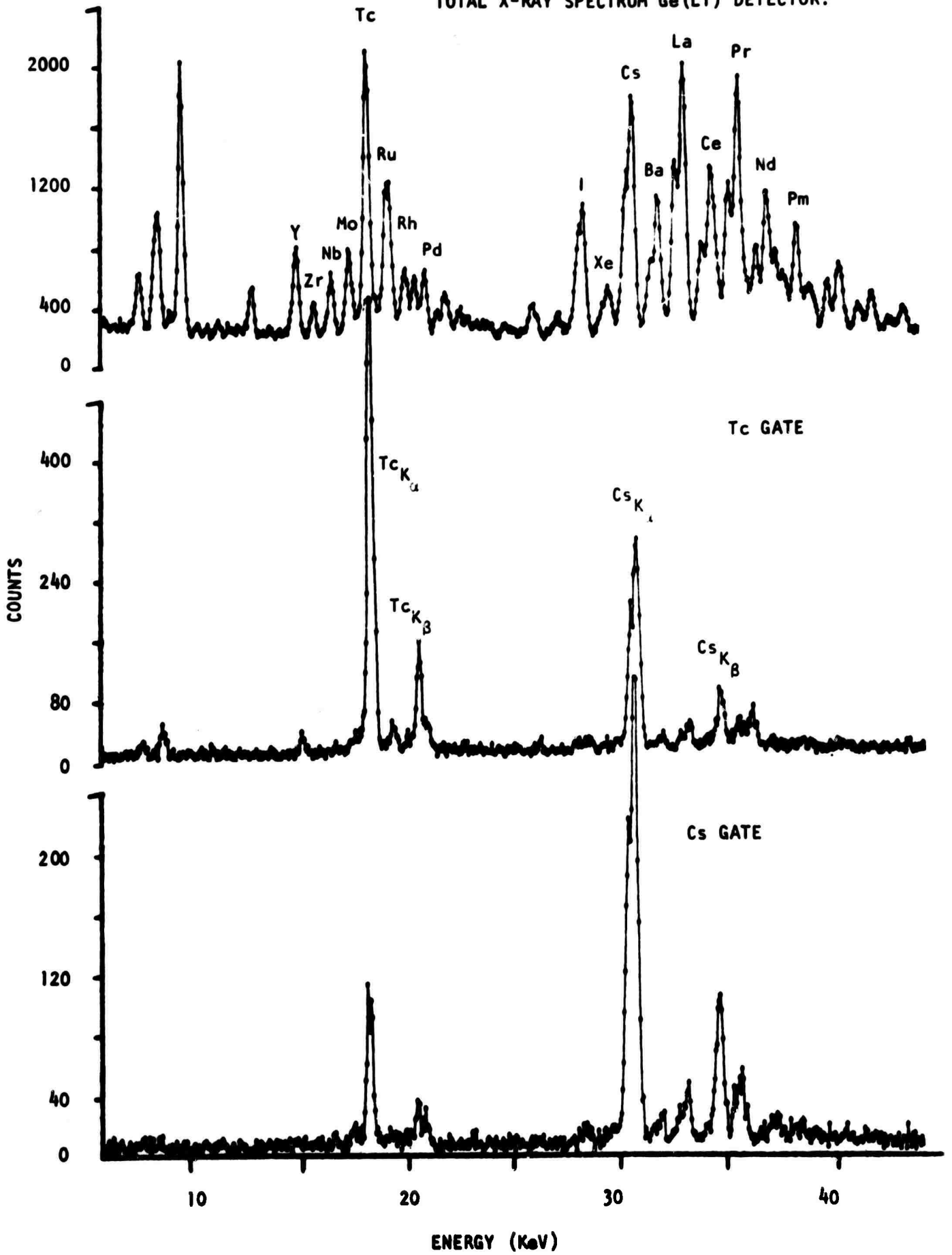
TOTAL X-RAY SPECTRUM Ge(Li) DETECTOR.



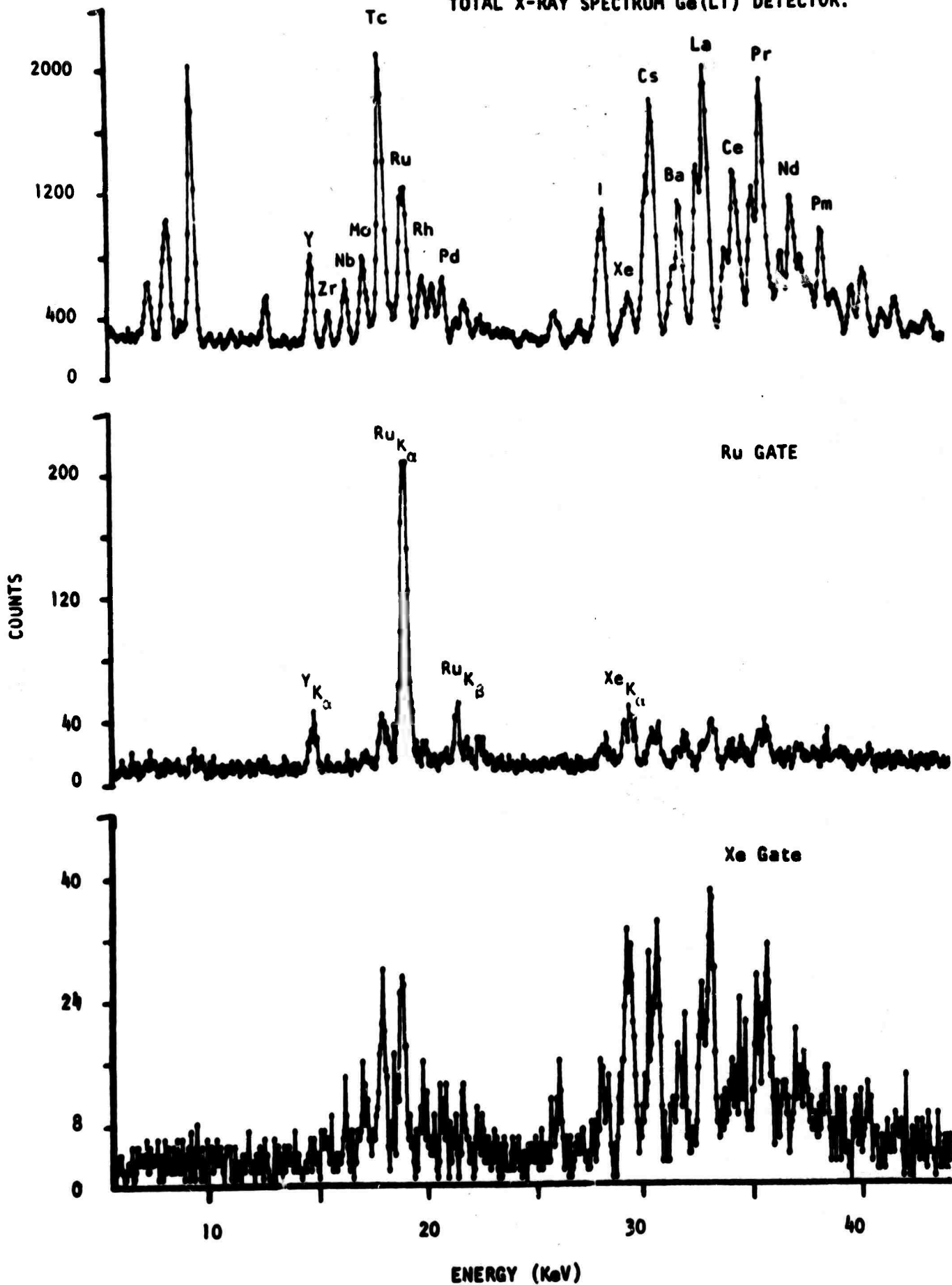
ENERGY (KeV)

032

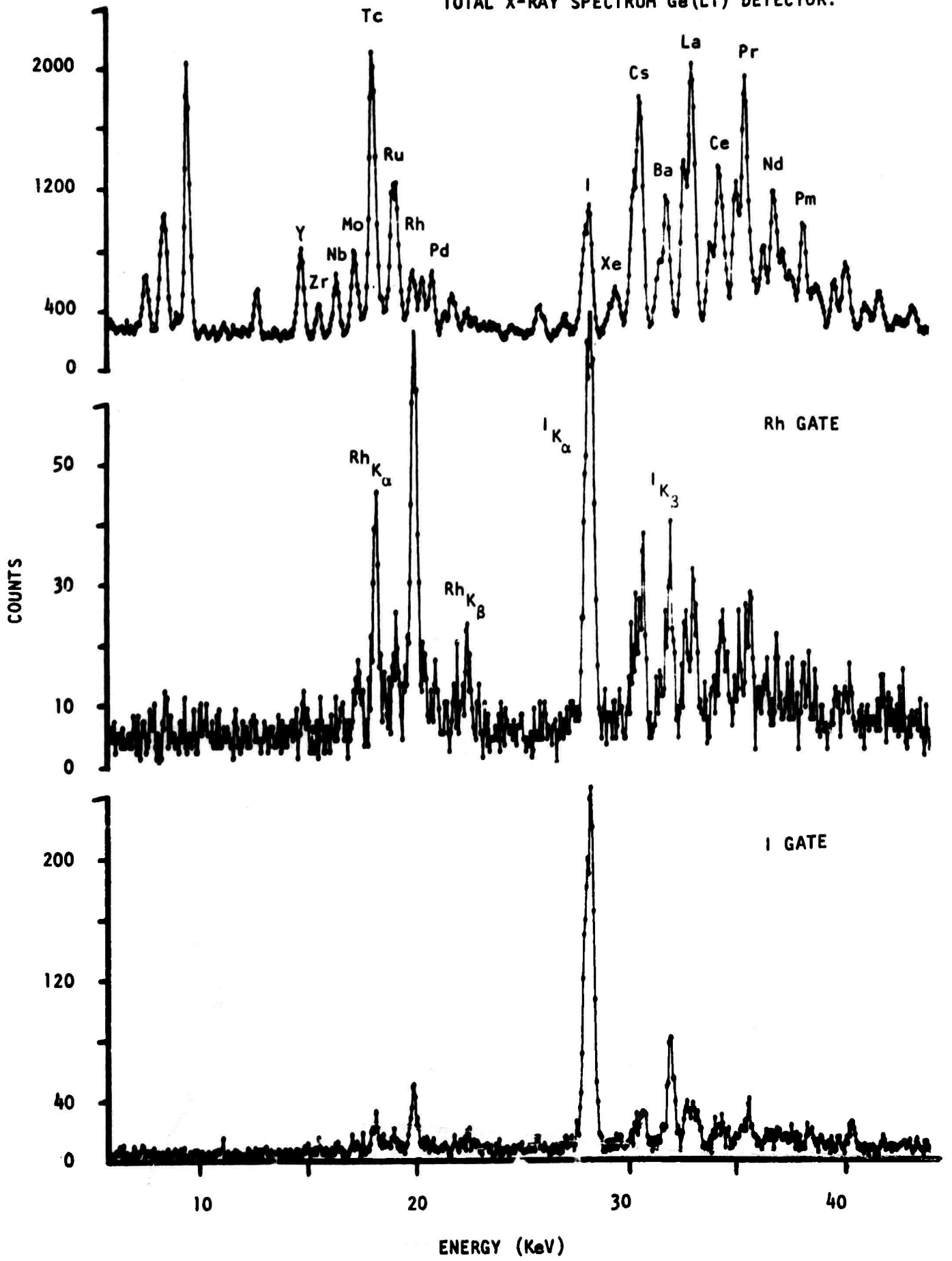
TOTAL X-RAY SPECTRUM Ge(Li) DETECTOR.

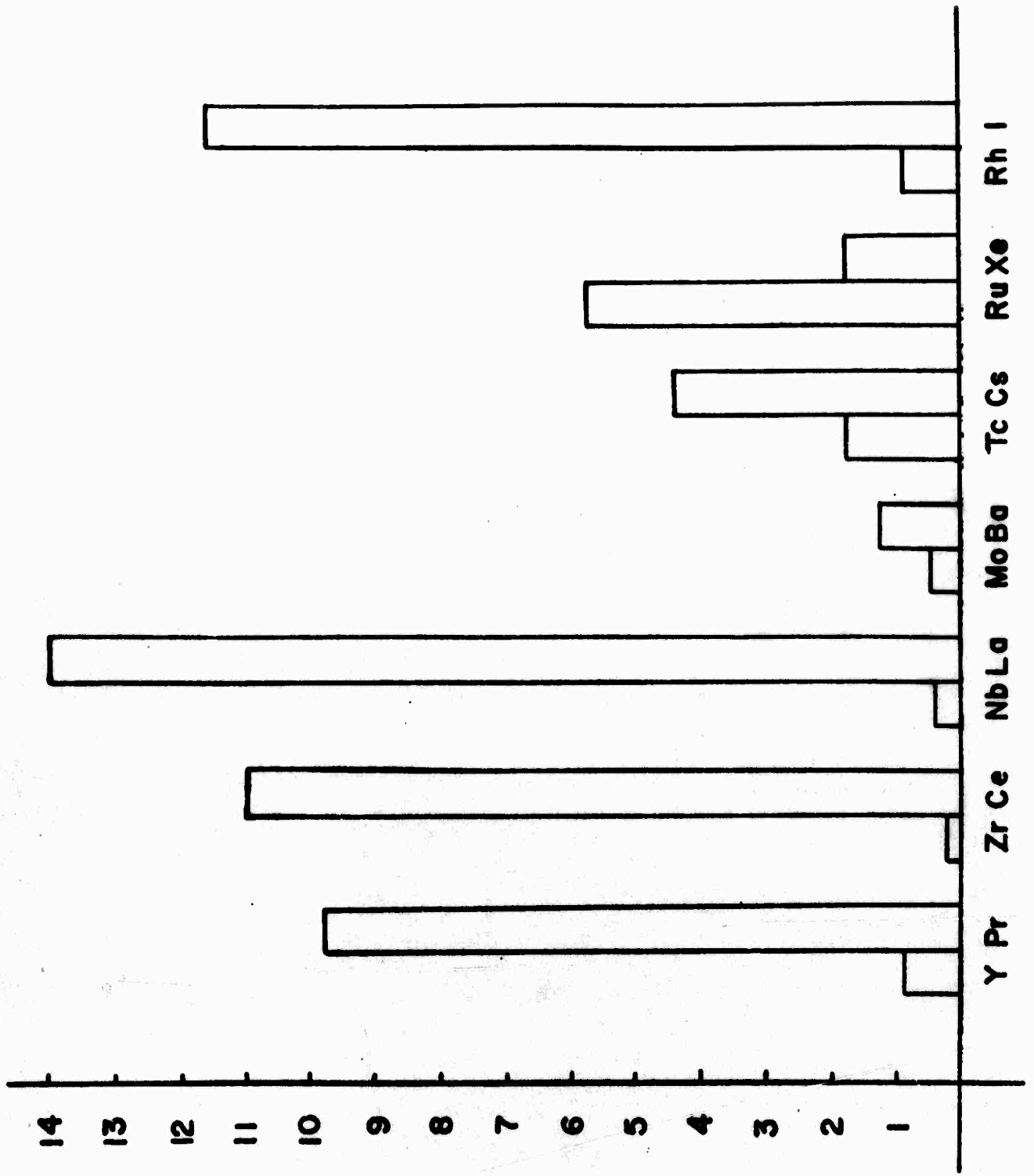


TOTAL X-RAY SPECTRUM Ge(LI) DETECTOR.



TOTAL X-RAY SPECTRUM Ge(Li) DETECTOR.





$\frac{(K_d \text{ self})}{(K_d \text{ comp})}$

## APPENDIX II

### LOW ENERGY TRANSITIONS FROM THE DE-EXCITATION OF SPONTANEOUS FISSION FRAGMENTS OF $^{252}\text{Cf}^*$

F. F. Hopkins, G. W. Phillips, J. R. White,  
C. F. Moore and P. Richard

Center for Nuclear Studies  
University of Texas at Austin 78712

#### ABSTRACT

Low energy  $\gamma$ -rays, in the range from 45 to 230 keV, following the spontaneous fission of  $^{252}\text{Cf}$ , are observed with a high resolution Ge(Li) detector (FWHM 500 eV at 81 keV), in coincidence with K X-rays from the fission fragments, observed with a Si(Li) detector (FWHM 350 eV at 31 keV). Sixteen 1024 channel gamma ray spectra were accumulated and sorted by computer, corresponding to windows set on K X-rays from Y, Zr, Nb, Mo, Tc, Ru, Rh, Pd, Pr, Ce, La, Ba, Cs, Xe, I, and Sb. In conjunction with previous works, this data allowed both mass and charge assignments to be made for a number of the observed  $\gamma$ -ray transitions.

## I. Introduction

The study of fission, both spontaneous and induced, has often involved coincidence techniques in attempts to correlate the various products. The myriad of states available to the system and the complexity of the decay schemes for the highly excited fragments present a rich source of information which is valuable both as a means of identifying the features of the scission process and as a means of studying the structure of the neutron-rich nuclei thereby produced, which are for the most part accessible in no other manner. The latter has received considerable attention in the case of the spontaneous fission of  $^{252}\text{Cf}$  from Cheifetz et al.,<sup>1</sup> Wilhelmy et al.,<sup>2</sup> and Watson et al.<sup>3</sup> These studies of coincidences between fission fragments, internal conversion electrons, X-rays, and/or  $\gamma$ -rays, have revealed much about deformed even-even nuclei in the populated regions.

The mass yields from binary fission of  $^{252}\text{Cf}$  have been determined with both coincidence and radiochemical methods.<sup>3,4</sup> In the former experiments, the resolution was about 2 u. A method devised by Schmitt et al.<sup>5</sup> to take into account pulse height effects in solid state detectors as well as neutron boil-off values from Bowman et al.<sup>6</sup> has allowed considerable confidence to be placed in recent mass calculations. The behavior of prompt neutrons, the correlations between the ensuing direct forms of decay,  $\gamma$ -radiation and internal conversion, and the mass yields have been investigated at length.<sup>3,6,7,8</sup> The work presented in this paper is concerned with observing low energy  $\gamma$ -transitions in the fragments from the spontaneous fission of  $^{252}\text{Cf}$  by use of an X-ray,  $\gamma$ -ray coincidence system. This is an effective tool in separating the many radiations involved. Such methods have been

used in studying higher energy transitions.<sup>9,10</sup> The continuing improvement in the resolutions of the available X-ray and  $\gamma$ -ray detectors, has made possible these measurements to a degree of accuracy heretofore unmatched.

## II. Experimental Setup

A 0.08  $\mu\text{Ci}$   $^{252}\text{Cf}$  source on a nickel backing was sandwiched between two 0.1 mm thick pieces of plastic on an aluminum aperture. The plastic stopped the fragments, thus providing a high coincidence rate and preventing Doppler distortions in the spectra. The source package was placed in contact with the beryllium window on the face of a thin window 0.14 cc Ge(Li) low energy photon detector and with the face of a 0.09 cc Si(Li) X-ray spectrometer about 2 cm away. This geometry provided optimum solid angles such that the count rate limitation of the Si counter, around 4000 counts/sec was reached. The actual resolutions of the respective detectors, 350 eV at the 31 keV line from a  $^{133}\text{Ba}$  source and 500 eV at the 81 keV line from the same source, were degraded somewhat by the electronics used as will be described below. Both detectors rested on pliant foundations to reduce pulses due to vibrations in the experimental environment.

Pulses from the detectors were routed through the timing and amplification circuitry presented in Fig. 1. The fast discriminators were set just above the low-level noise. The time-to-amplitude converter (TAC) was set at a full scale of 100 nsec, and the stop signal from the Ge counter was delayed 40 nsec. The time resolution of the system was 20 nsec FWHM. The TAC output was directed to a single-channel analyzer (SCA) which accepted

the 40-90 nsec segment of the total time spectrum which included practically all of the coincidence timing peak. The time requirement was roughly set at 50 nsec since lifetimes were not a major interest in this experiment. The output of the SCA provided a gate signal to allow the linear pulses to enter 1024 channel analog-to-digital converters (ADC).

The X-ray spectrum was calibrated by taking a self-gated  $^{252}\text{Cf}$  singles spectrum; the L X-rays from internal conversion in  $^{248}\text{Cm}$  following  $\alpha$ -decay of  $^{252}\text{Cf}$  provided a convenient source of known lines. The  $\gamma$ -ray spectrum was calibrated in a similar manner with  $^{57}\text{Co}$ ,  $^{133}\text{Ba}$ , and  $^{153}\text{Gd}$  sources each superimposed on the  $^{252}\text{Cf}$  spectrum to maintain count-rate conditions. Both energy calibrations were fit with third order polynomial functions. The total running time was about 10 days with a coincidence rate of about 50 counts/sec. The gains of the amplifiers were checked daily by simply restarting the total coincidence spectra and noting the locations of the prominent peaks. Fortunately no adjustments to the data were required, since no substantial gain drifts were encountered.

### III. Online Data Analysis

A PDP-7 computer was programmed to perform a two-parameter match-up between peaks in the X-ray and  $\gamma$ -ray spectra. The two-parameter program, initiated by a gate pulse at ADC1, accepted the linear pulses at ADC2 and ADC3 in either order. An additional pulse at the gate ADC before the other two had both received inputs would abort the current sequence and reinitiate the search. The coincident  $\gamma$ -rays were sorted and placed in corresponding

storage areas, according to windows set on the pertinent  $K_{\alpha_{1,2}}$  peaks in the X-ray spectrum. In this way the  $\gamma$ -rays from a particular set of isotopes and the complementary set of isotopes were separated from the radiation of the other fragments. Each gated spectrum was stored in 1024 channels located in the additional memory of a PDP-15 computer; an interprocessor buffer provided the access between the two computers.

#### IV. Results

The total coincidence X-ray spectrum in Fig. 2 consists of well separated  $K_{\alpha_{1,2}}$  X-ray peaks for the various fragments, with the light and heavy fragment groups centered about  $Z = 43$  (Tc) and  $Z = 55$  (Cs), respectively. The Ni and Ge X-rays in the low energy end of the spectrum were probably the result of  $\gamma$ -fluorescence of the nickel backing and the Ge crystal itself in coincidence with other  $\gamma$ -rays. The efficiency of this detector begins decreasing from 100% at about 15 keV and is about 30-35% in the region of the Cs peak. The intrinsic resolution of the Si(Li) system was degraded due to count rate effects. The "effective" resolution of the system was sufficient to allow sixteen well separated windows to be set accurately as shown in Fig. 3. The gates in each case were roughly equivalent to or slightly less than the FWHM for the  $K_{\alpha_{1,2}}$  peaks and, as is evident in the sorted data, allowed little overlapping between adjacent peaks. An additional concern in this arrangement was the location of  $K_{\beta}$  groups which in several instances were unresolved from neighboring  $K_{\alpha}$  groups. Specifically the Y, Zr, Nb, and Mo  $K_{\beta}$  X-rays were unresolved from the Nb, Mo, Tc, and Ru  $K_{\alpha}$

X-rays, respectively, in the light fragment region. The I, Xe, Cs, and Ba  $K_{\beta}$  lines overlapped with the Ba, La, Ce, and Pr  $K_{\alpha}$  X-rays, respectively, in the heavy fragment region. In such cases a comparison of the appropriate sorted spectra, taking into account the relative intensities of the  $\gamma$ -rays as well as the fact that the  $K_{\beta}$  X-rays were much weaker than most of the corresponding  $K_{\alpha}$  X-rays, reveals the extent of the overlap. Except for Pd and Sb, these settings recorded spectra for seven pairs of complementary fragments: Y-Pr, Zr-Ce, Nb-La, Mo-Ba, Tc-Cs, Ru-Xe, and Rh-I. The cross referencing within each pair proved highly informative in analyzing the data.

The total coincidence  $\gamma$ -spectrum which has 0.21 keV/channel, Fig. 4, has as its most noticeable features the large number of X-rays in the low-energy end and a 68.8 keV  $\gamma$ -ray which dominates the region of interest in this work, 45-230 keV. Energies below 45 keV lie in the range of some of the X-ray groups and so are open to ambiguity. The light fragment X-rays were only partially recorded whereas the heavy fragment group is entirely present, though compressed due to the gain. Immediately above this group is a series of closely spaced  $\gamma$ -rays of various intensities and energies, the strongest being the one at 68.8 keV. The efficiency of this detector, 100% at 60 keV, 50% at 80 keV, and dropping to 28% at 160 keV and about 20% at 220 keV, must be considered in order to get a true picture of the relative strengths.

The sorted  $\gamma$ -ray spectra corresponding to the windows on the light fragment X-rays and the complementary spectra from windows on the heavy fragment X-rays are shown in Figs. 5-11. Figs. 12 and 13 show the spectra

from windows on Pd and Sb X-rays, respectively, for which no complementary spectra were taken. The criterion for determining peaks was in a minimum of thirty counts above background in the peak channel and a somewhat Gaussian shape. Large single channel fluctuations were disregarded. The center of a given peak was estimated to the nearest quarter channel. The fit on the calibration was accurate to 0.1 keV and coupled with the error in the choice of the peak channel gave a total error of  $\pm 0.15$  keV. A point to note in each of the light fragment spectra is the predominance of the X-ray of each fragment's complement in the low energy end, a simple X-ray, X-ray coincidence arising from internal conversion in both fragments, which competes favorably with gamma decay in many of the low energy transitions.

Interestingly, each gate on a heavy fragment X-ray often saw an additional X-ray from that same fragment in the Ge detector. This self-coincidence demands two X-rays from the same fragment within a time span of about 50 nsec, an event which can arise from two internal conversions in the same cascade. This phenomenon is currently being investigated.<sup>11</sup>

The effects of gates on overlapping  $K_{\alpha}$  lines and unresolved  $K_{\beta}$ - $K_{\alpha}$  groups are noted by looking at the relative intensities of the peaks in the various spectra involved. The nature of the most heavily produced group of  $\gamma$ -rays, those seen by the gate on Technetium, is extremely helpful in this respect. The 68.8 keV  $\gamma$ -ray which dominates the total coincidence spectrum belongs to this group and is probably the transition assigned 69 keV by Watson et al.<sup>3</sup> in  $^{108}\text{Tc}$ . Any interference between gates in which Tc or its complement is involved can be gauged accurately by the strength

of this one line. It appears to a slight extent in all of the spectra, indicating a small background contribution. In the gated spectra from the adjacent Mo and Pd peaks, it is a bit stronger as should be expected. In total, however, it is obvious that this strongest group of lines has been well separated from the others.

The energies of the observed gamma rays are given in Table I, and the two spectra for each complementary set of fragments are compared with each other and with previous data. A few lines which did not quite qualify as peaks but which were definite possibilities are included in parentheses as are any quantities from other works which were reported doubtful. Also lines obviously due to overlap from adjacent spectra or from  $K_{\beta}$  X-rays have been omitted. Weaker lines have been included if evidence from relative intensities implies that they may be genuine. In many cases the combined information allows a definite assignment of mass and charge. In doubtful cases, where previous results disagree, the assignment is placed in parentheses.

There is generally excellent agreement with the data of Watson et al.<sup>3</sup> Seen in the present work are all low energy transitions in the appropriate ranges of mass and charge to which they give a confidence level of A or B. In a few cases the present data or the consensus of other references indicates the transition is from a fragment with charge adjacent to that assigned by them.

Agreement is also excellent with the data of John et al.<sup>7</sup> All low energy transitions in the mass range of the present work with halflives

less than 80 nsec are seen. However only three isomeric transitions are observed, and two of these are probably members of the same cascade. Since their gamma ray detector was shielded from the second fragment detector, this data gives a reliable indication as to whether the transitions occur in the light or the heavy fragment. Comparison with the work of Cheifetz et al.<sup>1</sup> and Wilhelmy et al.<sup>2</sup> on the decay of even-even nuclei reveals further agreement. This work also explains the weakness of the Xe and Tc X-rays, since the  $2^+-0^+$  transition energies for these isotopes are generally larger than the others, with correspondingly lower internal conversion probabilities.

Most of the low energy transitions seen by Alvager et al.<sup>12</sup> correspond well to values reported in this paper. Since a mass separator was used, this data generally gives the best mass values. There are two cases of apparent disagreement between Watson et al.<sup>3</sup> and Alvager et al.<sup>12</sup> on the one hand, and John et al.<sup>7</sup> on the other hand, as to whether the transition is from the light or the heavy fragment, possibly indicating doublets. The present data eliminates some ambiguities. For example, John et al.<sup>7</sup> observed a 97.5 keV, mass 150 gamma ray as well as a 98.3 keV, mass 101 gamma ray, either of which could have been the Zr-Ce 98 keV line. However the latter was attributed by them to be in the same gamma ray cascade as the 91 keV, mass 101 transition (see Table II) which the present data show to be from  $^{101}\text{Y}$ . Their use of lifetimes as a guide for grouping transitions in a cascade has been supported by the present data, which in every applicable instance assigns the  $\gamma$ -rays to the same nucleus. This implies the 98.3 keV line is also from  $^{101}\text{Y}$  and this is probably the line that Watson et al.<sup>3</sup> attributed

to a 99 keV transition in  $^{101}\text{Zr}$  but with a confidence level of C.

In the present data, the 112.4 keV gamma ray from Mo-Ba appears strong and sharp in both gates. The energy agrees very well with the gamma ray assigned to mass 104 by John et al.<sup>7</sup> The 119.6 keV gamma ray from Tc-Cs is seen weakly in both spectra. Again the energy agrees well with the gamma ray assigned mass 109 in the same work.

Where they overlap, there is generally little correlation between the present work and the previous gamma ray data of Rueggsegger, Jr. et al.<sup>9</sup> and Eddy et al.;<sup>10</sup> however the latter works covered mainly higher energy gamma rays which lie beyond the energy range of the detector used in the present work.

## V. Discussion

The de-excitation process in each primary fragment is culminated by a  $\gamma$ -cascade and possibly internal conversion. In a given binary fission event, one of the two post-neutron fragments or both can emit X-rays as well as  $\gamma$ -rays, as depicted in Fig. 14. An X-ray,  $\gamma$ -ray coincidence requirement does not limit the event to a direct one, as a delayed cascade-internal conversion sequence in a beta-decay product is accepted under this format. The three possibilities, X-ray from one primary fragment and  $\gamma$ -ray from the other, X and  $\gamma$  from the same primary fragment, and X and  $\gamma$  from a beta decay chain member can be separated to an extent by a comparison of the data for gates on two complementary X-rays. A  $\gamma$ -ray appearing in both spectra must be associated with a prompt event some of the time, since a delayed

$\gamma$ -ray would not be in coincidence with an X-ray from the complementary fragment even though it is not certain which is the complementary fragment. However, it is possible, but not necessary, that some of the time,  $\gamma$ -ray can be associated with a delayed event in self coincidence with its cascade internal conversion X-ray. Table I demonstrates the great number of these lines which must be direct in some events. It also indicates that most of the gamma rays assigned to a specific fragment are in coincidence with X-rays from both that fragment and its complement, or from only the complement, implying a direct transition. The lifetime data of John et al.<sup>7</sup> generally support this conclusion. An unidentified  $\gamma$ -ray seen in only one of the spectra could arise from a direct or delayed event.

Excluding those instances where  $\gamma$ -rays have been matched with the data of earlier experiments for a particular Z value, no distinction can be made on the basis of this data between the complementary fragments as possible sources of the radiation. This problem can be resolved only by allowing separation of the fragments by free flight and thereby greatly degrading the geometry.

A gamma-ray from a given fragment will appear in the spectrum gated by X-rays from that fragment, if it is in coincidence with one or more cascade transitions having an appreciable probability for internal conversion. This situation can result from low transition energy or a high multipolarity. However, generally a multipolarity greater than E2 will result in a half-life too long for coincidence with a preceding transition. These features are illustrated in Table II which gives the  $2^+ - 0^+$  ground state band transitions

observed in the even-even nuclei and the  $4^+-2^+$  transitions in these bands, according to the data of Cheifetz et al.<sup>1</sup> and Wilhelmy et al.<sup>2</sup> Also given are the nature of the transitions observed in the present data, and the internal conversion probabilities  $P_K$  defined in terms of the coefficients  $\alpha_K$ , tabulated by Hager and Seltzer,<sup>13</sup>

$$P_K = \frac{\alpha_K}{1+\alpha_K} .$$

$P_K$  is the probability for K-shell internal conversion, neglecting higher shell contributions. For the odd Z nuclei, Table II gives the energy and half-life of transitions attributed to the same cascade by John et al.,<sup>7</sup> which are observed in the present data, and the  $P_K$  for E1, M1, or E2 transitions.

The  $2^+-0^+$  transitions in the even-even nuclei are all observed in the spectrum gated on the complementary X-rays, but the only line seen strongly in the self-gated spectrum is from <sup>150</sup>Ca, which has the lowest energy  $4^+-2^+$  transition, with by far the largest  $P_K$ . The transitions in the odd Z nuclei seem to follow the same trend, as exhibited by the range for  $P_K$  over the probable multipolarities, i.e., a  $\gamma$ -ray is seen in the self-gated spectrum when there is evidence that it is in coincidence with a transition with an appreciable internal conversion probability.

A reasonable assumption to make in analyzing this data is that the majority of the strong low energy lines arise from transitions between low-lying states; states higher in excitation would in general tend to emit higher energy radiation. In particular, the comparison of the spectra for the even Z groups with the even-even data of Cheifetz et al.<sup>1</sup> and Wilhelmy et al.<sup>2</sup>

suggests that practically all of these low energy  $\gamma$ -rays are coming from even Z - odd A nuclei, in accordance with expectations from nuclear structure. The odd-even and odd-odd nuclei similarly would be expected to give rise to a multitude of low-lying closely-spaced states; the odd Z spectra accordingly display a profusion of low energy lines. In addition, the odd Z - X-rays predominate in the total coincidence spectrum; the relative intensities of the X-ray peaks in this spectrum are very similar to those in the prompt coincidence spectra of Watson et al.<sup>14</sup> and therefore support the assertion that many of the X-rays and  $\gamma$ -rays seen in this experiment are prompt. The predominance in the X-ray production of odd Z over even Z heavy fragments was attributed by the same work to closed shell effects in the Z=50, N=82 region. The present work indicates less of an effect for the light fragments, for which the neutron levels, in the general range N=58 to N=68, are well-removed from any major closed shell.

The preconditions for the substantial amount of internal conversion contributing to the decay schemes of these fragments, small energy spacings or large spin differences, were recorded in gross spectra by Kapoor et al.<sup>15</sup> and Kleinheinz and Siegbahn.<sup>16</sup> The former group found that roughly 57% of the X-rays from <sup>252</sup>Cf fission fragments represent halflives from 0.1 to 1.0 nsec and 23% are emitted from 1.0 to 50 nsec. The latter work revealed that the lifetimes for transitions 130 to 260 keV in energy are to a large extent compatible with M1 or enhanced E2 transitions. The specific lifetimes reported by Watson et al.<sup>3</sup> for the transitions seen in this work are also in the 1 to 2 nsec range. All of this data concurs with the present data in the fact that a large number of the  $\gamma$ -transitions are M1 or E2 in origin and so, coupled

with small transition energy, would give rise to a large number of X-rays as well as low energy  $\gamma$ -rays.

Although quite a few assignments of  $\gamma$ -rays to a specific mass and charge were possible in this work, many of the strong low energy lines have not been seen in previous work and so remain unidentified as to mass. The limitations on the data of John et al.<sup>7</sup> prevented further matching of  $\gamma$ -rays. They analyzed only the strongest lines below 80 keV, omitted the 70-80 keV segment due to lead X-rays, and recorded  $\gamma$ -rays emitted a minimum of 3 nsecs after fission. Transitions reported here which are direct and fall within their energy range but which they failed to see are probably somewhat less than 3 nsec in lifetime. The lower energy  $\gamma$ -rays were simply beyond the capabilities of their 9 cm<sup>3</sup> Ge(Li) detector. An experiment involving  $\gamma$ -ray fragment mass coincidence is planned as a supplement to this work, and those results will be used to complete the identifications.

## References

\* This research was supported in part by the Advanced Research Projects Agency of the Department of Defense and was monitored by the Office of Naval Research under Contract No. N00014-67-A-0126-0012 and was supported in part by the U. S. Atomic Energy Commission.

1. E. Cheifetz, R. C. Jared, S. G. Thompson, and J. B. Wilhelmy, Phys. Rev. Lettrs. 25, 38(1970).
2. J. B. Wilhelmy, S. G. Thompson, R. C. Jared, and E. Cheifetz, Phys. Rev. Lettrs. 25, 1122(1970).
3. R. L. Watson, J. B. Wilhelmy, R. C. Jared, C. Ruge, H. R. Bowman, S. G. Thompson, and J. O. Ras-ussen, Nucl. Phys. A141, 449(1970).
4. W. E. Nervik, Phys. Rev. 119, 1685(1960).
5. H. W. Schmitt, W. E. Kiker, and C. W. Williams, Phys. Rev. 137, B837(1965).
6. H. R. Bowman, J. C. D. Milton, S. G. Thompson, and W. J. Swiatecki, Phys. Rev. 126, 2120(1962); 2133(1963).
7. W. John, F. W. Gay, and J. J. Wesolowski, Phys. Rev. C2, 1451(1970).
8. H. Nifenecker, J. Frehaut, and M. Soleilhac, Proc. IAEA Conference on the Physics and Chemistry of Fission (Vienna, Austria, 1969) IAEA Vienna, 491(1965).
9. D. R. Ruegsegger, Jr., and R. R. Roy, Phys. Rev. C1, 631(1970).
10. N. W. Eddy and R. R. Roy, Phys. Rev. C3, 877(1971).
11. R. St Laurent et al., to be published.
12. T. Alvager, R. A. Naumann, R. F. Petry, G. Sidenius, and T. D. Thomas, Phys. Rev. 167, 1105(1968).

13. R. S. Hager and E. C. Seltzer, Nucl. Data A4, 1(1968).
14. R. L. Watson, H. R. Bowman, and S. G. Thompson, Phys. Rev. 162, 1169(1967).
15. S. S. Kapoor, H. R. Bowman, and S. G. Thompson, Phys. Rev. 140, B1310(1965).
16. P. Kleinheinz and K. Siegbahn, Nucl. Phys. A90, 145(1967).

TABLE I  
YTTRIUM, PRAESODYNIUM

Present		Others		Assigned	
$E_Y$ (keV)		$E_Y$ (keV)	Mass	$E_Y$ (keV)	Mass
Y	Pr				
	48.6				
	52.5				
54.8	54.8				
58.2	58.3				
65.5		65 <sup>a</sup>	( <sup>150</sup> Pr)	65.5	<sup>150</sup> Pr
	68.9				
	71.7				
	74.2	74 <sup>a</sup>	<sup>150</sup> Pr	74.2	<sup>150</sup> Pr
	76.6				
	79.9				
82.3	81.9				
	87.6				
90.8	90.8	91.5 <sup>b,k</sup>	<sup>101</sup> <sub>-1</sub> <sup>+0</sup>	91.0	<sup>101</sup> Y
95.1					
96.2	98.2	98.3 <sup>b,k</sup>	<sup>101</sup> <sub>-0</sub> <sup>+1</sup>	98.2	<sup>101</sup> Y
		99 <sup>a</sup>	( <sup>101</sup> Zr)		
100.5	100.7				
102.7					
	103.4				
109.2		109.4 <sup>b</sup>	150±0	109.3	<sup>150</sup> Pr
119.3					

YTTRIUM, PRAESODYNIUM Cont'd

Present		Others		Assigned	
$E_Y$ (keV)		$E_Y$ (keV)	Mass	$E_Y$ (keV)	Mass
Y	Pr				
	122.6	122.0 <sup>b</sup>	$99^{+1}_{-0}$	122.3	$99_Y$
	125.2				
130.2	130.2				
	134.5				
158.2	(158)				

ZIRCONIUM, CERIUM

Present		Others		Assigned	
$E_{\gamma}$ (keV)		$E_{\gamma}$ (keV)	Mass	$E_{\gamma}$ (keV)	Mass
Zr	Ce				
	48.0				
	52.2				
53.6	53.2				
55.0	54.7				
	58.0				
	59.1				
64.3	64.3				
	70.2				
	75.2				
82.8					
	87.3				
98.2	98.0	97.1 <sup>c,d,k</sup>	$^{150}_{\text{Ce}}$	97.7	$^{150}_{\text{Ce}}$
		97.5 <sup>b</sup>	$150 \pm 1$		
		99 <sup>a</sup>	( $^{101}_{\text{Zr}}$ )		
	104.0	103.2 <sup>b,h,l</sup>	$^{150}_{-1}^{+0}$	103.6	$^{150}_{\text{Ce}}$
117.8	117.6				
121.6					
130.2	(130)	130.9 <sup>b,h,l</sup>	$150 \pm 0$	130.6	$^{150}_{\text{Ce}}$
133.8	133.4	135.4 <sup>b,g</sup>	$^{148}_{-0}^{+1}$	134.0	$^{148}_{\text{Ce}}$
	(135.9)				
	(141.1)				
143.1	142.4	143 <sup>a</sup>	$^{149}_{\text{Pr}}$		

ZIRCONIUM, CERIUM Cont'd

Present		Others		Assigned	
$E_{\gamma}$ (keV)		$E_{\gamma}$ (keV)	Mass	$E_{\gamma}$ (keV)	Mass
Zr	Ce				
		142.6 <sup>b</sup>	$149_{-1}^{+0}$	142.7	$149_{\text{Ce}}$
		145.2 <sup>f</sup>			
	151.5	151.9 <sup>d</sup>	$102_{\text{Zr}}$	151.8	$102_{\text{Zr}}$
		152.1 <sup>b</sup>	$101_{-0}^{+1}$		
		153 <sup>a</sup>	$102_{\text{Zr}}$		
158.8	(158.4)	155.7 <sup>f</sup>			
		158.7 <sup>c</sup>	$148_{\text{Ce}}$	158.7	( $148_{\text{Ce}}$ )
		158.8 <sup>b</sup>	$147_{-1}^{+0}$		
		158 <sup>a</sup>	$148_{\text{Ce}}$		
	209.5	209 <sup>d,k</sup>	$150_{\text{Ce}}$	209.5	$150_{\text{Ce}}$
	213.1	212.7 <sup>d</sup>	$100_{\text{Zr}}$	212.9	$100_{\text{Zr}}$
		214.8 <sup>f</sup>			

NIOBIUM, LANTHANUM

Present		Others		Assigned	
$E_{\gamma}$ (MeV)		$E_{\gamma}$ (MeV)	Mass	$E_{\gamma}$ (MeV)	Mass
Nb	La				
46.9	46.4				
56.2	56.0				
58.1	57.9	58.3 <sup>b,k</sup>	147±2	58.1	147 <sub>La</sub>
61.2					
	62.8				
64.5	64.2	64 <sup>a</sup>	146 <sub>La</sub>	64.3	146 <sub>La</sub>
66.2	65.9				
67.1	66.9				
72.1					
73.6					
	74.0				
77.6	77.6				
81.1					
82.1	81.8	82.8 <sup>b,1</sup>	146 <sup>+1</sup> <sub>-0</sub>	82.2	146 <sub>La</sub>
84.4	84.0				
91.2	90.8				
97.0	96.9				
100.3	99.6	100 <sup>a</sup>	(145 <sub>La</sub> )	100.0	145 <sub>La</sub>
102.0					
104.0	103.7	105.0 <sup>b</sup>	146±2	104.3	146 <sub>La</sub>
106.7					
	114.8				

NIOBIUM, LANTHANUM Cont'd

Present		Others		Assigned	
E <sub>γ</sub> (MeV)		E <sub>γ</sub> (MeV)	Mass	E <sub>γ</sub> (MeV)	Mass
Nb	La				
119.5	119.1				
125.0					
126.4	126.1				
130.7	130.4	130.5 <sup>b</sup>	146±0	130.6	146 <sub>La</sub>
		131 <sup>a</sup>	146 <sub>La</sub>		
	135.8				
	140.9	140.9 <sup>b</sup>	104±0	140.9	104 <sub>Nb</sub>
	(144.5)	144.1 <sup>b</sup>	104±1	144.3	104 <sub>Nb</sub>
	150.4				
	153.8				
	156.8				
159.3	158.8	158.8 <sup>b,k</sup>	147 <sup>+0</sup> <sub>-1</sub>	158.9	(147 <sub>La</sub> )
		158 <sup>a</sup>	148 <sub>Ce</sub>		
	162.1				
	(164.1)	164.2 <sup>b</sup>	130±0	164.2	103 <sub>Nb</sub>
167.7	167.5	167.7 <sup>b,1</sup>	146 <sup>+1</sup> <sub>-0</sub>	167.7	146 <sub>La</sub>
172.2	172.0	175.0 <sup>e</sup>		172.2	
	182.8				

MOLYBDENUM, BARIUM

Present		Others		Assigned	
$E_{\gamma}$ (keV)		$E_{\gamma}$ (keV)	Mass	$E_{\gamma}$ (keV)	Mass
Mo	Ba				
45.3					
48.4					
50.1					
58.1					
64.3					
65.9	66.4				
94.8	94.9	95 <sup>a</sup>	<sup>106</sup> Mo	94.9	<sup>106</sup> Mo
	98.2				
102.4	102.7	100.9 <sup>j</sup>	141	102.5	<sup>141</sup> Ba
109.8	110.0	109.7 <sup>b</sup>	145±2	109.8	<sup>145</sup> Ba
112.4	112.6			112.4	( <sup>104</sup> Mo)
		113 <sup>a</sup>	<sup>144</sup> Ba		
		112.3 <sup>b</sup>	104±0		
		113.4 <sup>j</sup>	141		
117.2	117.6	117.3 <sup>b</sup>	144±1	117.3	( <sup>142</sup> Ba)
		118 <sup>a</sup>	<sup>140</sup> Cs		
		118.7 <sup>j</sup>	141		
		117.9 <sup>j</sup>	142		
137.8	138.0	137.7 <sup>j</sup>	141	137.9	<sup>141</sup> Ba
144.8	144.7	(144.1) <sup>b,g</sup>	<sup>104</sup> <sub>-0</sub> <sup>+1</sup>	144.7	( <sup>104</sup> Mo)
152.1	152.1	(151) <sup>a</sup>	<sup>106</sup> Mo	152.1	<sup>106</sup> Mo

1. 050

MOLYBDENUM, BARIUM Cont'd

Present		Others		Assigned	
E <sub>γ</sub> (keV)		E <sub>γ</sub> (keV)	Mass	E <sub>γ</sub> (keV)	Mass
Mo	Ba				
154.3					
	155.0				
	164.9				
(171.7)	171.9	172 <sup>2</sup>	<sup>106</sup> Mo	171.9	<sup>106</sup> Mo
		171.7 <sup>d</sup>	<sup>106</sup> Mo		
		172.2 <sup>b</sup>	106±0		
181.4		183 <sup>a</sup>	<sup>144</sup> Ba	181.4	( <sup>145</sup> Ba)
		181.0 <sup>c</sup>	<sup>146</sup> Ba		
		183.5 <sup>b,g</sup>	145±1		
	193.0	192 <sup>a</sup>	<sup>106</sup> Mo	193.0	( <sup>105</sup> Mo)
		192.3 <sup>d</sup>	<sup>104</sup> Mo		
		193.6 <sup>b</sup>	105±0		
200.0		199 <sup>a</sup>	<sup>144</sup> Ba	199.6	<sup>144</sup> Ba
		198.4 <sup>j</sup>	142		
		199.4 <sup>c</sup>	<sup>144</sup> Ba		

TECHNETIUM, CESIUM

Present		Others		Assigned	
$E_{\gamma}$ (keV)		$E_{\gamma}$ (keV)	Mass	$E_{\gamma}$ (keV)	Mass
Tc	Cs				
	45.5				
46.1					
	49.1				
50.3					
51.0	50.7				
54.1					
	54.5				
55.1					
58.2	58.0				
	59.5				
61.7	61.5	61 <sup>a</sup>	<sup>140</sup> Cs	61.6	<sup>140</sup> Cs
62.3					
64.4	64.1				
	66.8				
68.8	69.0	69 <sup>a</sup>	<sup>108</sup> Tc	68.9	<sup>108</sup> Tc
71.6	71.4	69.4 <sup>j</sup>	141	71.5	<sup>141</sup> Cs
76.7	76.5	74.6 <sup>j</sup>	141	76.5	<sup>141</sup> Cs
78.7	78.5	78 <sup>a</sup>	<sup>140</sup> Cs	78.6	<sup>140</sup> Cs
80.1	79.9	79.4 <sup>j</sup>	<sup>140</sup> Cs	80.0	<sup>140</sup> Cs
81.9	81.5	81.8 <sup>j</sup>	141	81.7	<sup>141</sup> Cs
84.3	84.1				
85.7	85.4	85.6 <sup>b,k</sup>	<sup>105</sup> <sub>-0</sub> <sup>+1</sup>	85.6	<sup>105</sup> Tc

TECHNETIUM, CESIUM Cont'd

Present		Others		Assigned	
$E_{\gamma}$ (keV)		$E_{\gamma}$ (keV)	Mass	$E_{\gamma}$ (keV)	Mass
Tc	Cs				
	86.2				
	88.9				
90.2		89.7 <sup>j</sup>	141		
		90.5 <sup>b,1</sup>	142±0	90.3	<sup>142</sup> Cs
91.1	91.6	92.1 <sup>j</sup>	<sup>142</sup> Cs	91.4	<sup>142</sup> Cs
96.7		97.0 <sup>b,1</sup>	142±0	96.9	<sup>142</sup> Cs
	102.8	102.8 <sup>b,k</sup>	105±0	102.8	<sup>105</sup> Tc
104.6					
106.1	105.9	106.1 <sup>j</sup>	141	106.0	<sup>141</sup> Cs
		106.0 <sup>b</sup>	142±2		
108.1	107.8				
	109.8				
	115.1	115.6 <sup>b,m</sup>	109±0	115.4	<sup>109</sup> Tc
119.7	119.5	118 <sup>a</sup>	<sup>140</sup> Cs	119.6	<sup>109</sup> Tc
		119.4 <sup>b,m</sup>	109±0		
		118.7 <sup>j</sup>	141		
123.2	122.9	123 <sup>a</sup>	<sup>109</sup> Tc	123.1	<sup>109</sup> Tc
125.0	124.5				
137.3	136.8				
138.3	138.3	138.3 <sup>j</sup>	138	138.3	<sup>138</sup> Cs
154.0	154.3	154.3 <sup>j</sup>	138	154.1	<sup>138</sup> Cs
161.7		161.5 <sup>f</sup>			

RUTHENIUM, XENON

Present		Others		Assigned)	
E <sub>γ</sub> (keV)		E <sub>γ</sub> (keV)	Mass	E <sub>γ</sub> (keV)	Mass
Ru	Xe				
50.7	50.6				
	58.1				
63.0					
70.8					
	71.7	72 <sup>a</sup>	<sup>110</sup> Ru	71.7	<sup>110</sup> Ru
74.2	74.3				
	76.6				
	81.9				
82.6					
	94.7				
96.2		96.2 <sup>b,h</sup>	<sup>110</sup> <sub>-1</sub> <sup>+0</sup>	96.2	<sup>110</sup> Ru
98.3	98.4	98 <sup>a</sup>	<sup>108</sup> (Tc)	98.3	<sup>108</sup> Ru
100.7					
102.7	102.6				
104.0	(104.1)	103.5 <sup>b</sup>	<sup>111</sup> <sub>-1</sub> <sup>+0</sup>	103.7	<sup>111</sup> Ru
108.6					
117.8					
131.9		131.8 <sup>b</sup>	110±0	131.8	<sup>110</sup> Ru
138.3					
142.7					
143.4					
150.5		150 <sup>a</sup>	( <sup>110</sup> Ru)	150.5	( <sup>111</sup> Ru)
		150.5 <sup>b</sup>	111±0		

RHODIUM, IODINE

Present		Others		Assigned	
$E_Y$ (keV)		$E_Y$ (keV)	Mass	$E_Y$ (keV)	Mass
Rh	I				
45.7	45.6				
	49.8	49 <sup>a</sup>	116 <sub>Rh</sub>	49.8	116 <sub>Rh</sub>
52.8					
	57.1				
58.8	58.8	59 <sup>a</sup>	136 <sub>I</sub>	58.8	136 <sub>I</sub>
60.5	60.6	60.5 <sup>b</sup>	121±1	60.5	112 <sub>Rh</sub>
65.8	65.5				
	68.3				
82.5	82.3				
87.4	87.4	(88) <sup>a</sup>	136 <sub>I</sub>	87.4	136 <sub>I</sub>
91.5					
96.0					
(112.1)	112.1				
116.8	116.8				
	118.3				
137.8					
	155.3	155.0 <sup>b</sup>	137±0	155.1	137 <sub>I</sub>
	158.9				
159.5	159.8				
	161.4				
	162.1				
	212.7				
	230.2				

**PALLADIUM**

**Present**

**$E_{\gamma}$  (keV)**

48.6

58.3

178.5

## ANTIMONY

Present

$E_{\gamma}$  (keV)

45.8

58.3

60.7

65.7

71.2

75.2

76.6

81.8

82.5

91.8

125.4

126.0

138.3

<sup>a</sup>See Ref. 3. (Energy uncertainty  $\sim \pm 1$  keV).

<sup>b</sup>See Ref. 7. (Energy uncertainty  $\sim \pm 0.2$  keV).

<sup>c</sup>See Ref. 2. (Energy resolution  $\sim 1$  keV at 122 keV).

<sup>d</sup>See Ref. 1. (Energy resolution  $\sim 1$  keV at 122 keV).

<sup>e</sup>See Ref. 9. (Energy uncertainty  $\sim \pm 3$  keV).

<sup>f</sup>See Ref. 10. (Energy uncertainty  $\sim \pm 3$  keV).

<sup>g</sup>May be Doppler shifted according to Ref. 7.

<sup>h</sup>Isomeric transition ( $t_{1/2} > 80$  nsecs) from Ref. 7.

<sup>j</sup>See Ref. 12. (Energy uncertainty  $\sim \pm 1.5$  keV to  $\pm 2.0$  keV).

<sup>klm</sup>Identify pairs of  $\gamma$ -rays attributed to the same cascade by Ref. 7.

TABLE II  
LOW ENERGY CASCADE TRANSITIONS

Even-Even Nuclei						
	$E_{\gamma}$ (keV) <sup>a</sup>		2 <sup>±</sup> 0 <sup>+</sup> Observed?		$P_K^{2^+}$ (E2)	$P_K^{4^+}$ (E2)
	2 <sup>±</sup> 0 <sup>+</sup>	4 <sup>±</sup> 2 <sup>+</sup>	Complimentary gated	Self gated		
<sup>110</sup> Zr	152	327	yes	(wk)	0.18	0.014
<sup>102</sup> Zr	213	352	yes	(wk)	0.05	0.009
<sup>148</sup> Ce	159	300	yes	(wk)	0.23	0.04
<sup>150</sup> Ce	97	209	yes	yes	0.58	0.11
<sup>104</sup> Mo	172	351	yes	wk	0.13	0.012
<sup>144</sup> Ba	199	331	yes	no	0.12	0.0?
<sup>146</sup> Ba	181	333	yes	no	0.16	0.03

Odd Z Nuclei							
	$E_{\gamma}$ <sup>b</sup> (keV)	$\gamma_{1/2}$ <sup>c</sup>	Observed?		(E1)	$P_K$ (M1)	(E2)
			Complimentary gated	Self gated			
<sup>101</sup> Y	91.0	19	yes	yes	0.1	0.2	0.6
	98.2	21	yes	yes	0.1	0.2	0.5
<sup>146</sup> La	82.2	13	yes	yes	0.2	0.7	0.7
	167.7	16	yes	yes	0.04	0.1	0.2
<sup>147</sup> La	58.1	8	yes	yes	0.5	0.8	0.8
	158.9	10	yes	yes	0.05	0.2	0.2
<sup>105</sup> Tc	85.6	16	wk	yes	0.2	0.4	0.6
	102.8	15	yes	no	0.1	0.2	0.5
<sup>109</sup> Tc	115.4	18	yes	(wk)	0.08	0.2	0.4
	119.6	16	yes	yes	0.07	0.1	0.4
<sup>142</sup> Cs	90.3	15	yes	yes	0.2	0.5	0.6
	96.9	16	yes	no	0.2	0.4	0.6

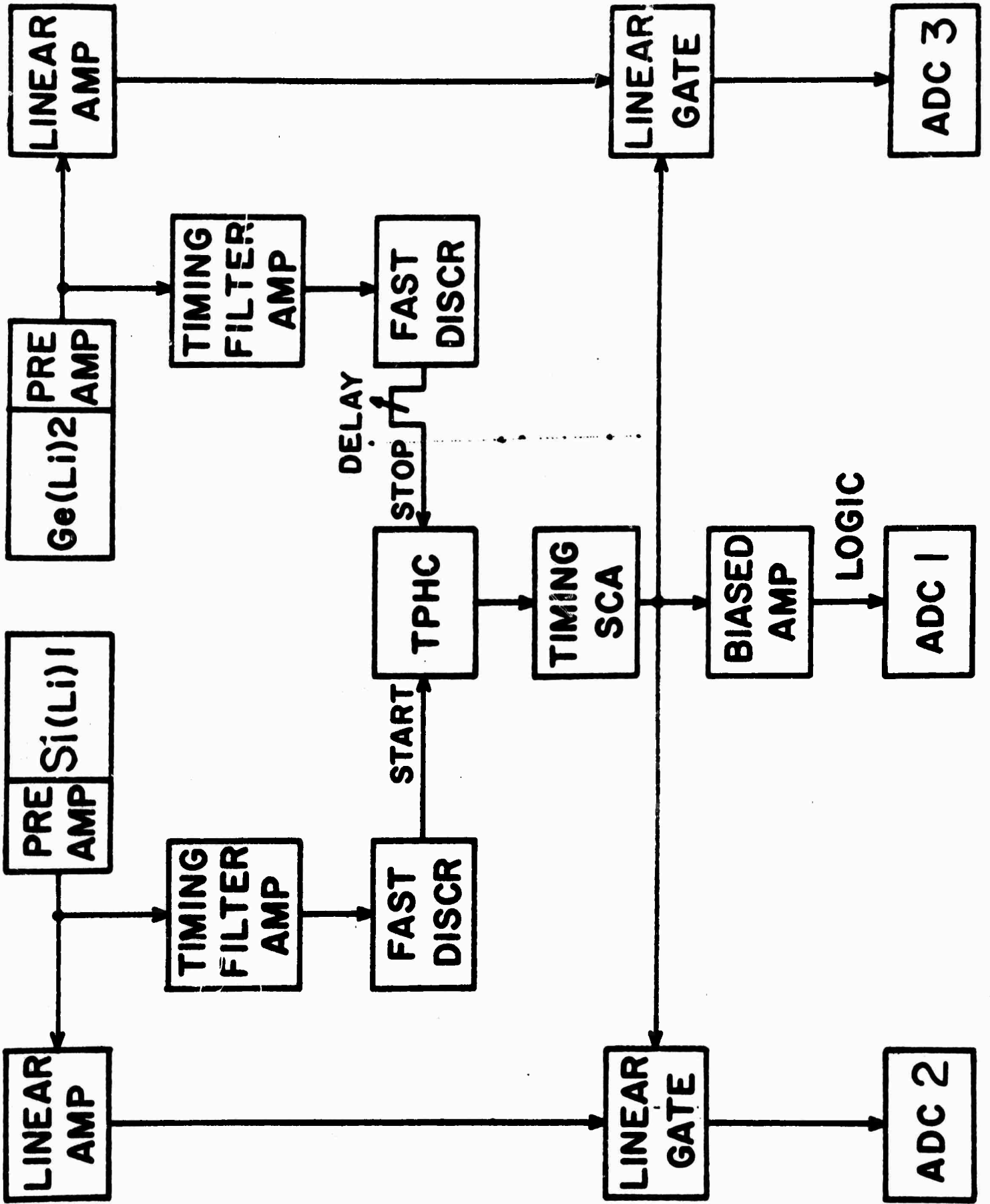
<sup>a</sup>See Refs. 1 and 2.

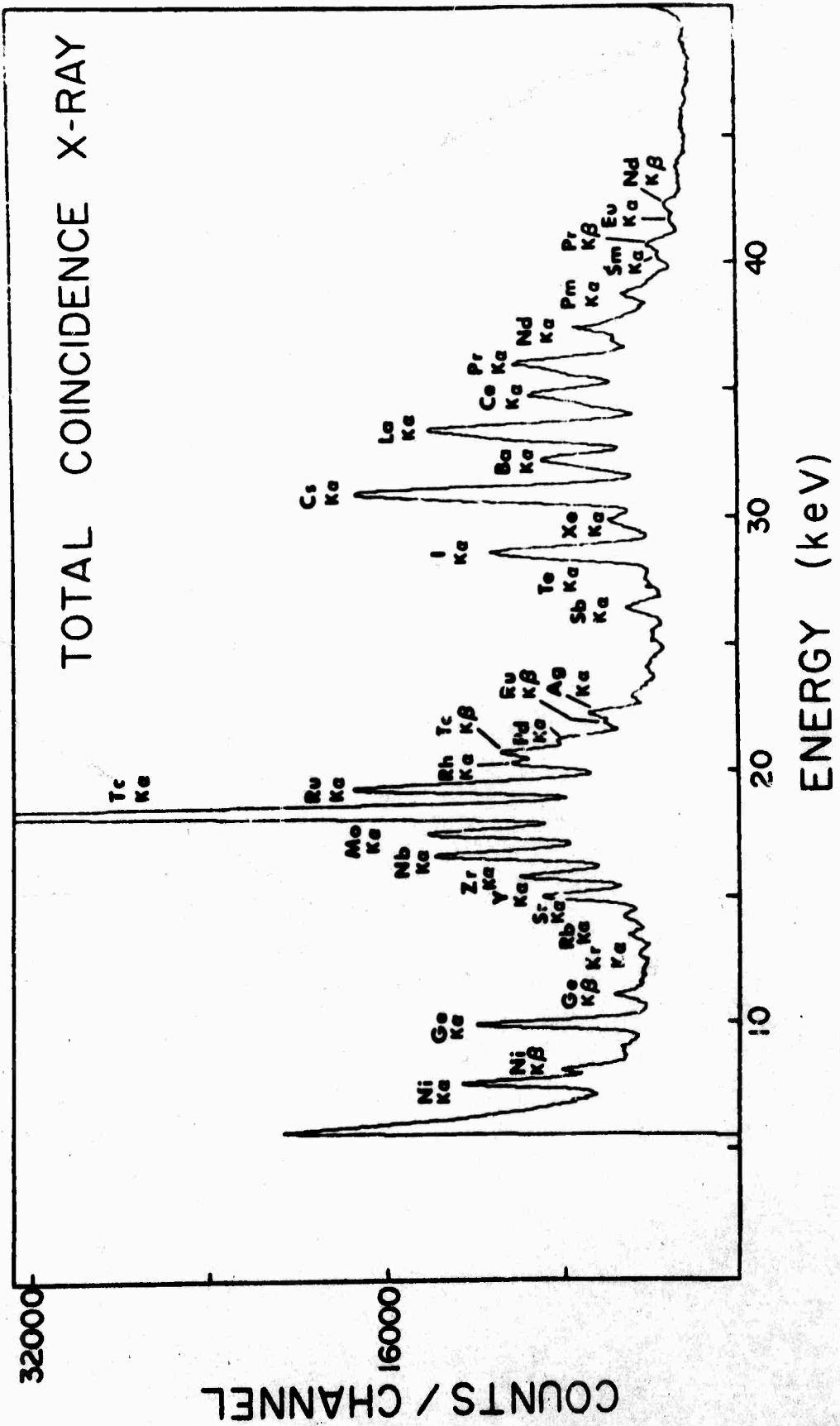
<sup>c</sup>See Ref. 7.

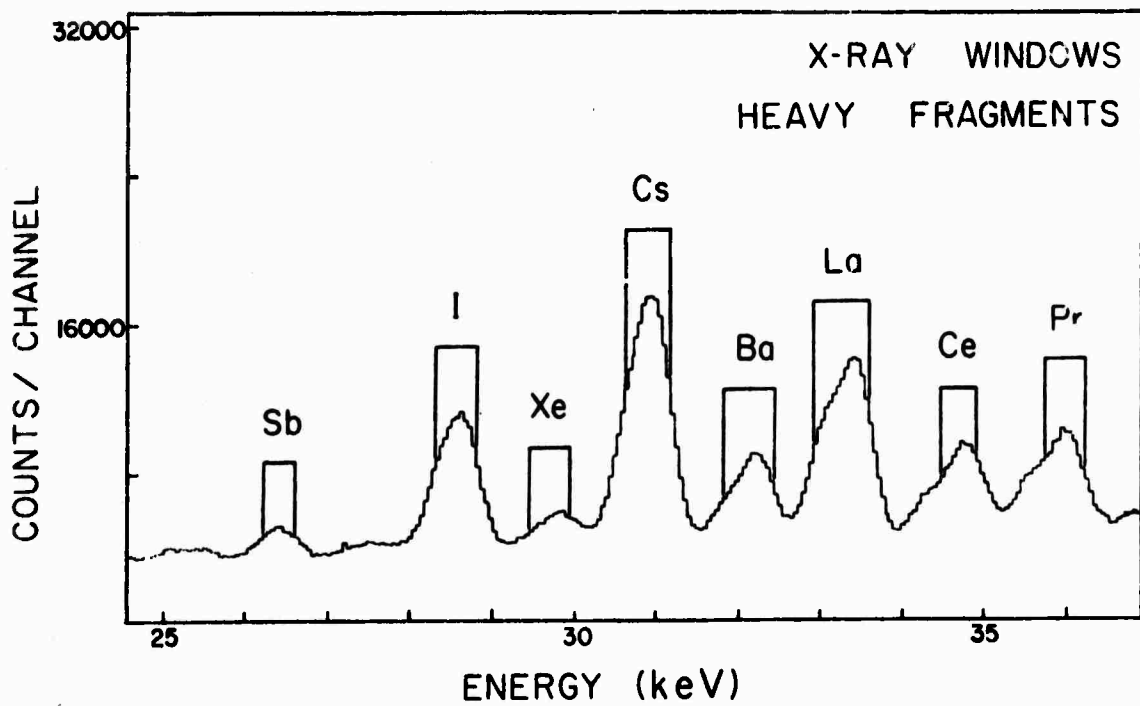
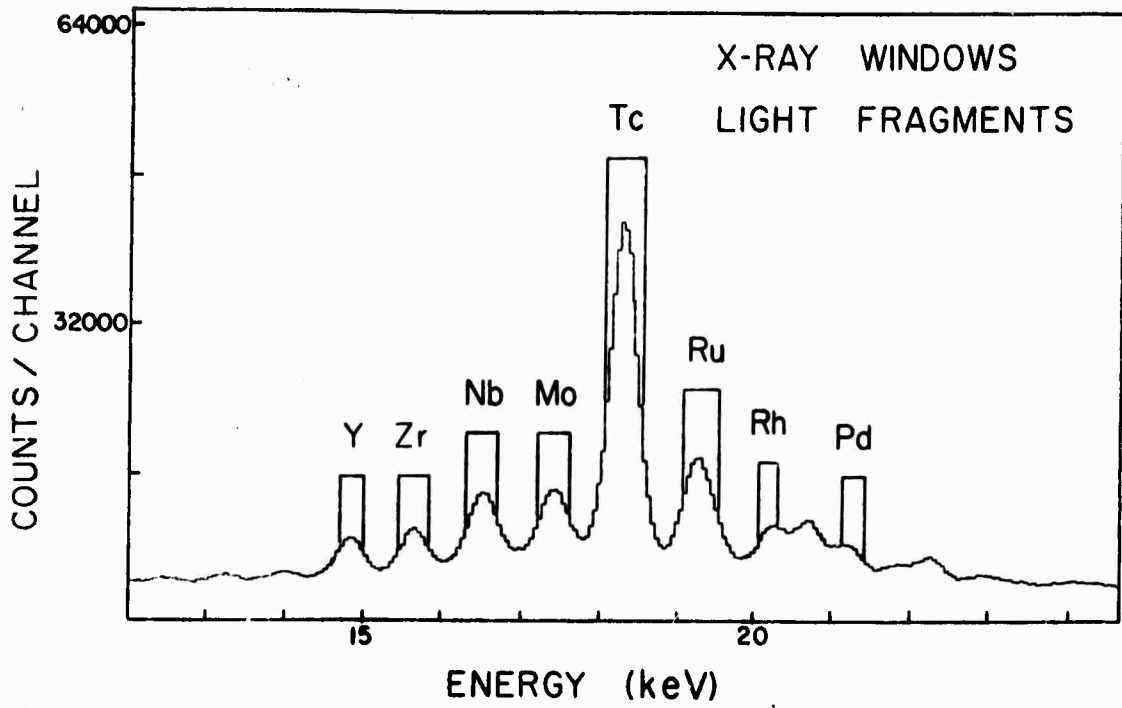
<sup>b</sup>Energies in this work presented as final values.

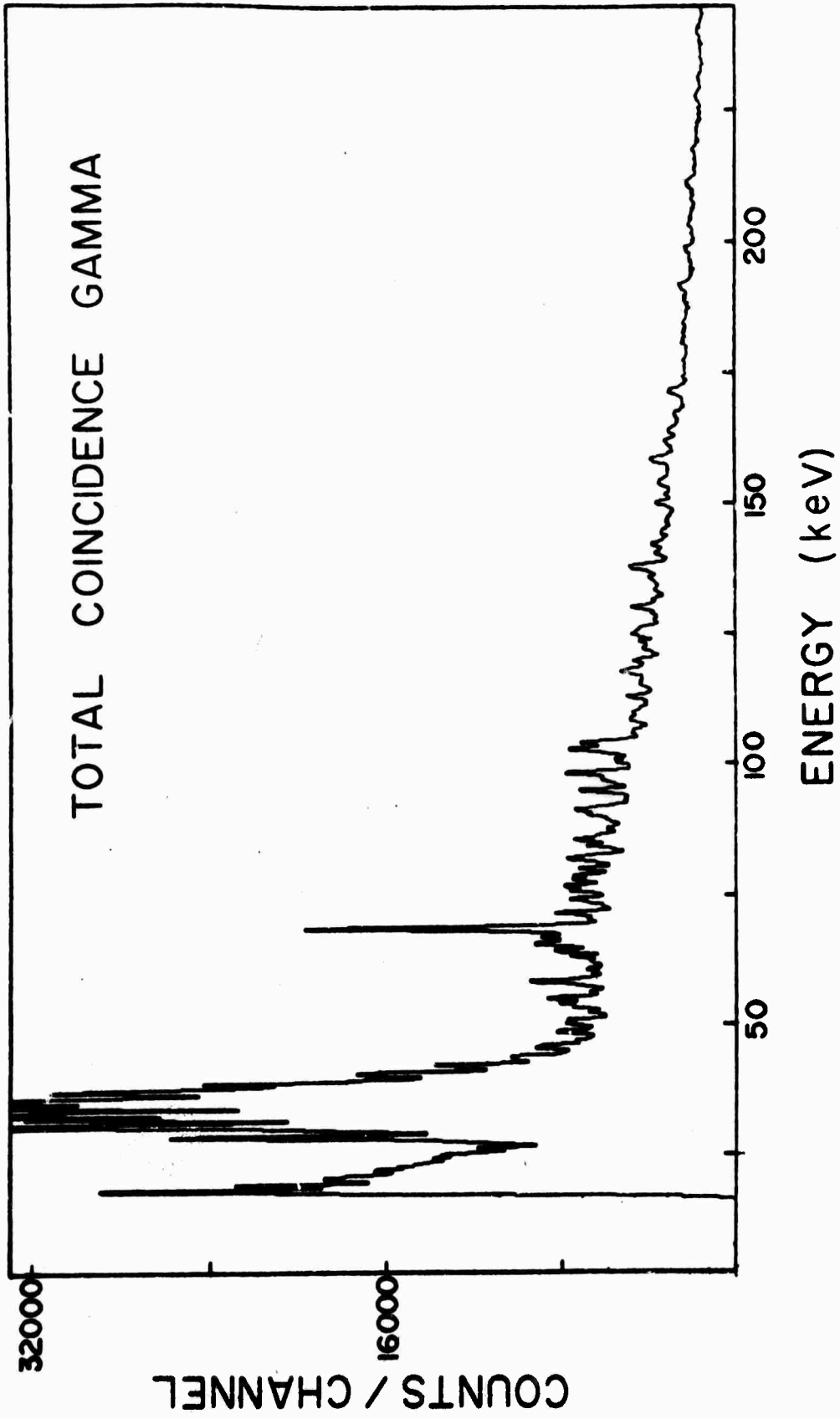
### Figure Captions

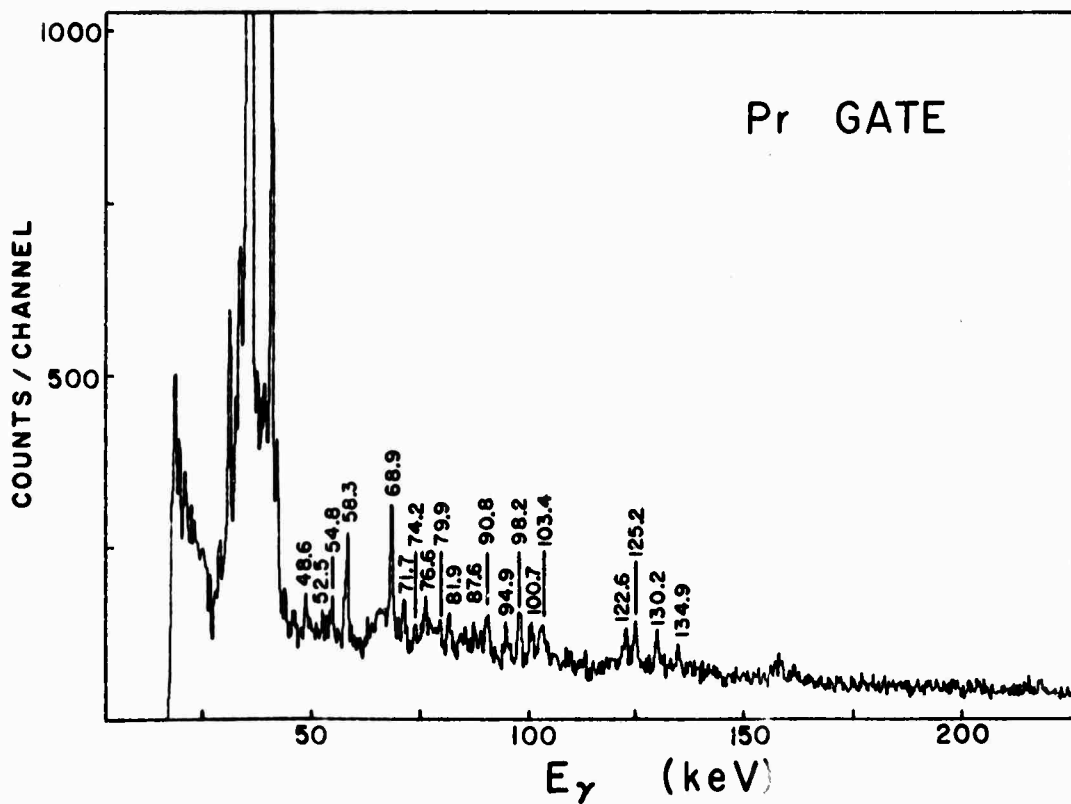
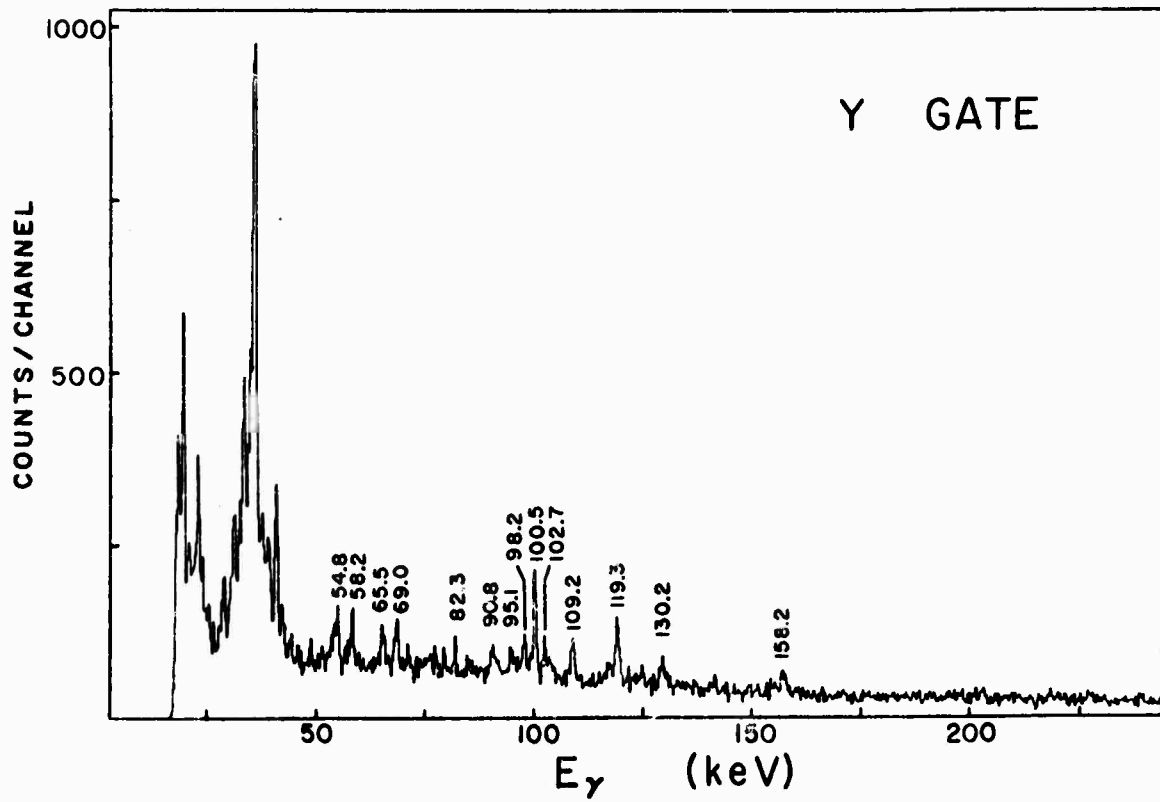
- Fig. 1 Schematic diagram of electronics.
- Fig. 2 Total coincidence X-ray spectrum.
- Fig. 3 (a) Windows set on X-rays from light fragments. (b) Windows set on X-rays from heavy fragments.
- Fig. 4 Total coincidence  $\gamma$ -ray spectrum.
- Fig. 5 (a) Sorted  $\gamma$ -ray spectrum from gate on yttrium. (b) Sorted  $\gamma$ -ray spectrum from gate praseodymium.
- Fig. 6 (a) Sorted  $\gamma$ -ray spectrum from gate on zirconium. (b) Sorted  $\gamma$ -ray spectrum from gate on cerium.
- Fig. 7 (a) Sorted  $\gamma$ -ray spectrum from gate on niobium. (b) Sorted  $\gamma$ -ray spectrum from gate on lanthanum.
- Fig. 8 (a) Sorted  $\gamma$ -ray spectrum from gate on molybdenum. (b) Sorted  $\gamma$ -ray spectrum from gate on barium.
- Fig. 9 (a) Sorted  $\gamma$ -ray spectrum from gate on technetium. (b) Sorted  $\gamma$ -ray spectrum from gate on cesium.
- Fig. 10 (a) Sorted  $\gamma$ -ray spectrum from gate on ruthenium. (b) Sorted  $\gamma$ -ray spectrum from gate on xenon.
- Fig. 11 (a) Sorted  $\gamma$ -ray spectrum from gate on rhodium. (b) Sorted  $\gamma$ -ray spectrum from gate on iodine.
- Fig. 12 Sorted  $\gamma$ -ray spectrum from gate on palladium.
- Fig. 13 Sorted  $\gamma$ -ray spectrum from gate on antimony.
- Fig. 14 Generalized decay scheme for lower levels in the fission fragments.
- All of the indicated modes of X-ray -  $\gamma$ -ray coincidences were accepted in the system used in this experiment.

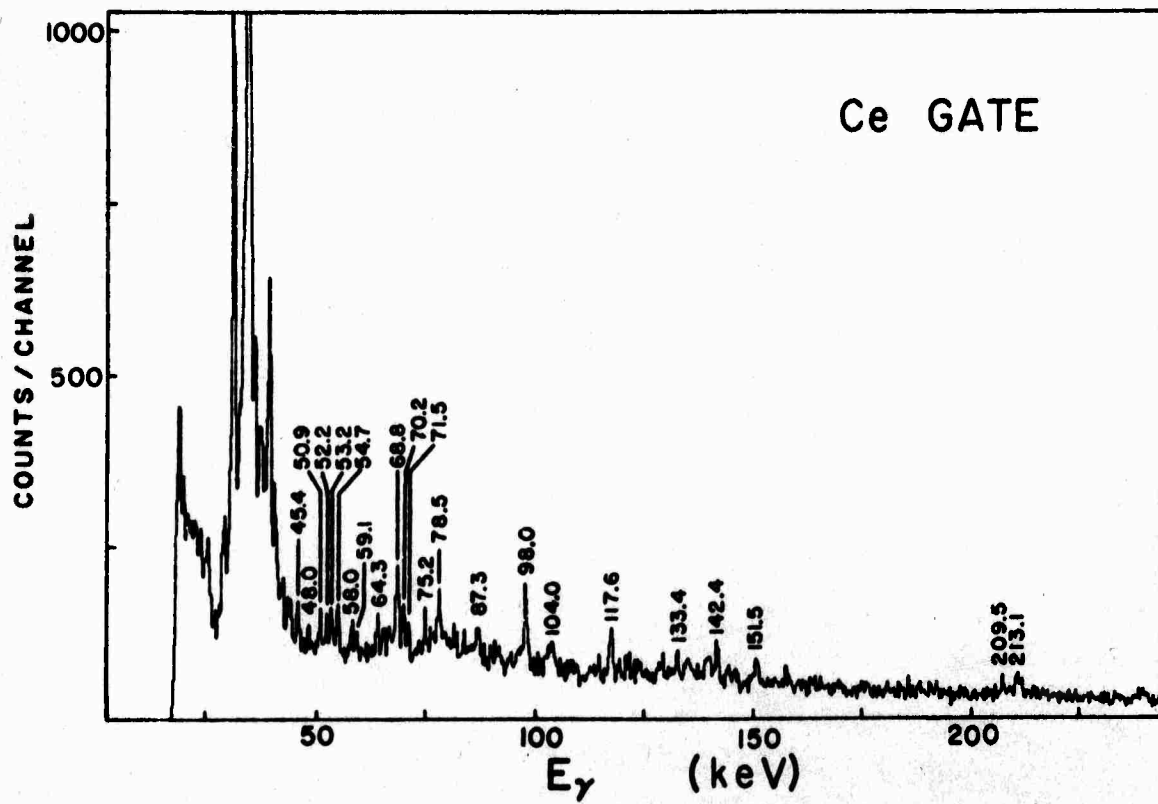
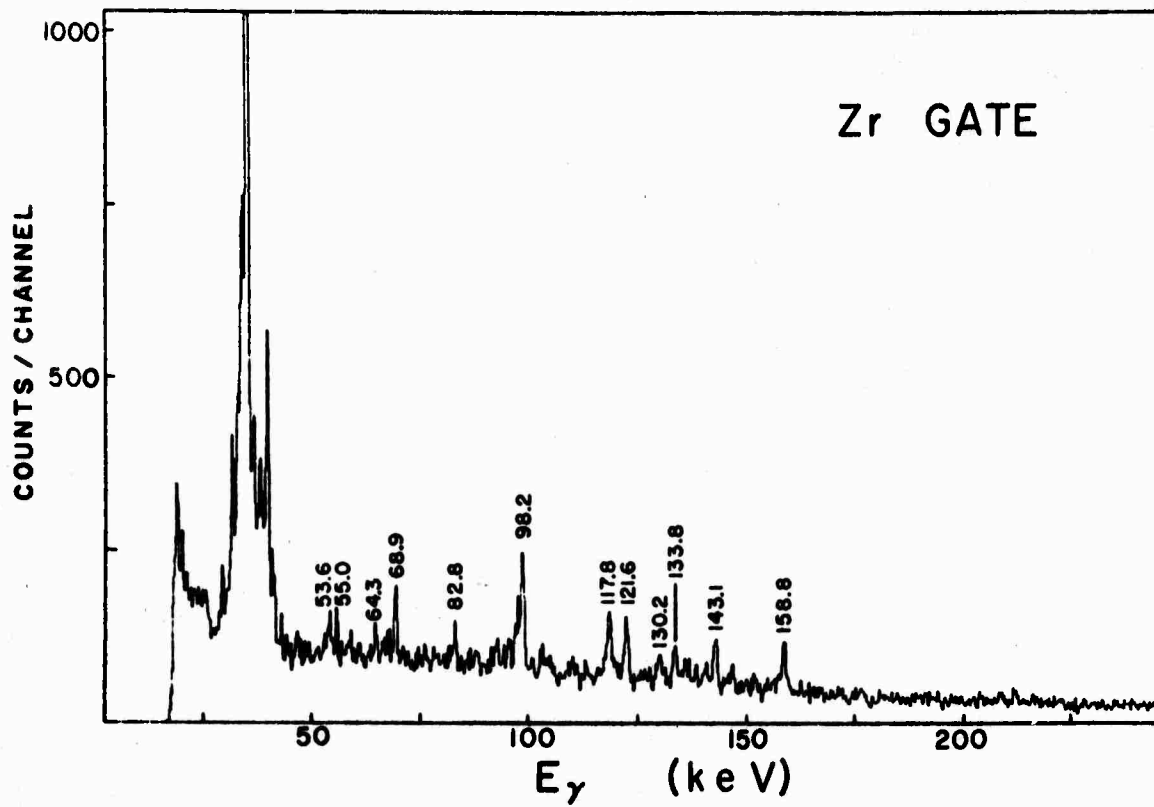


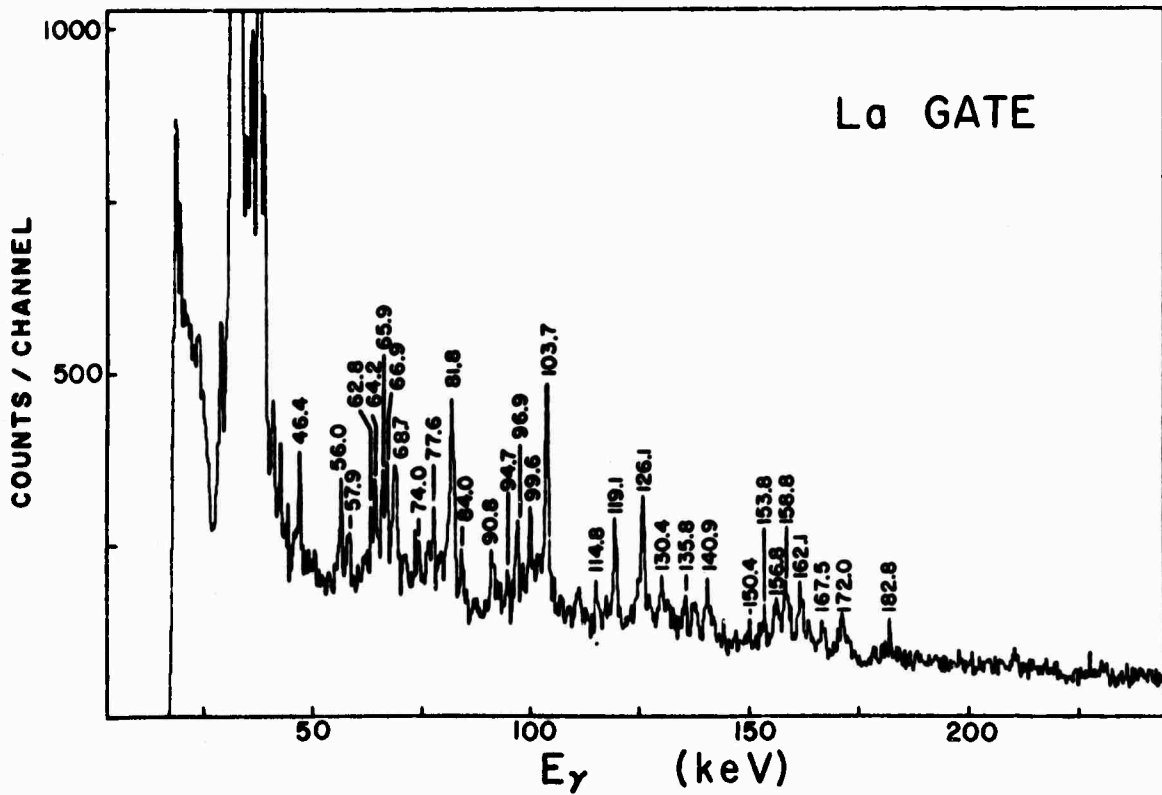
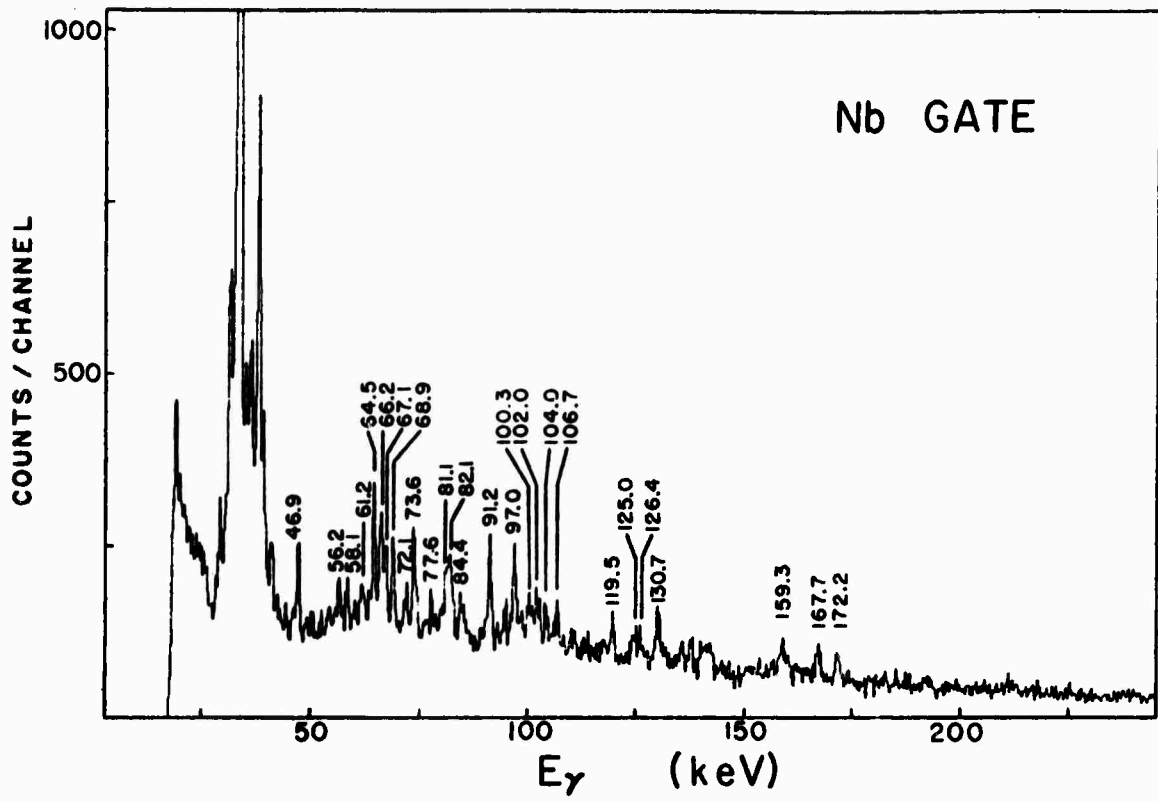


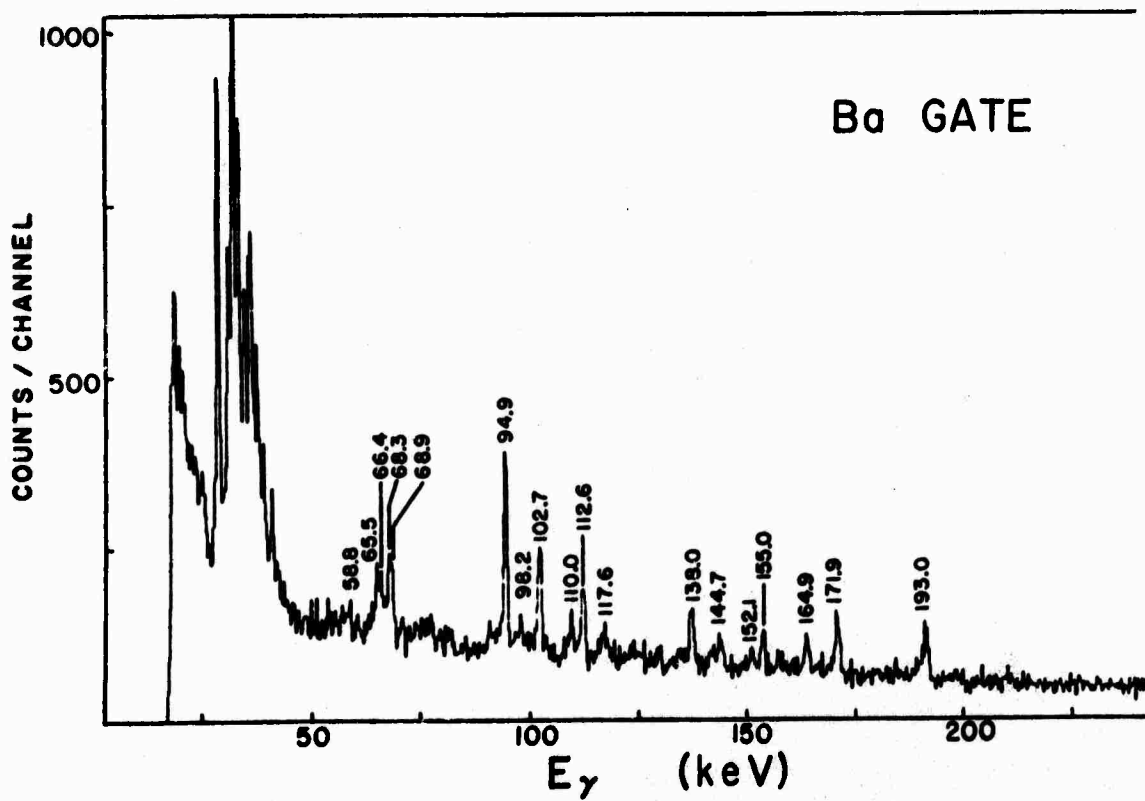
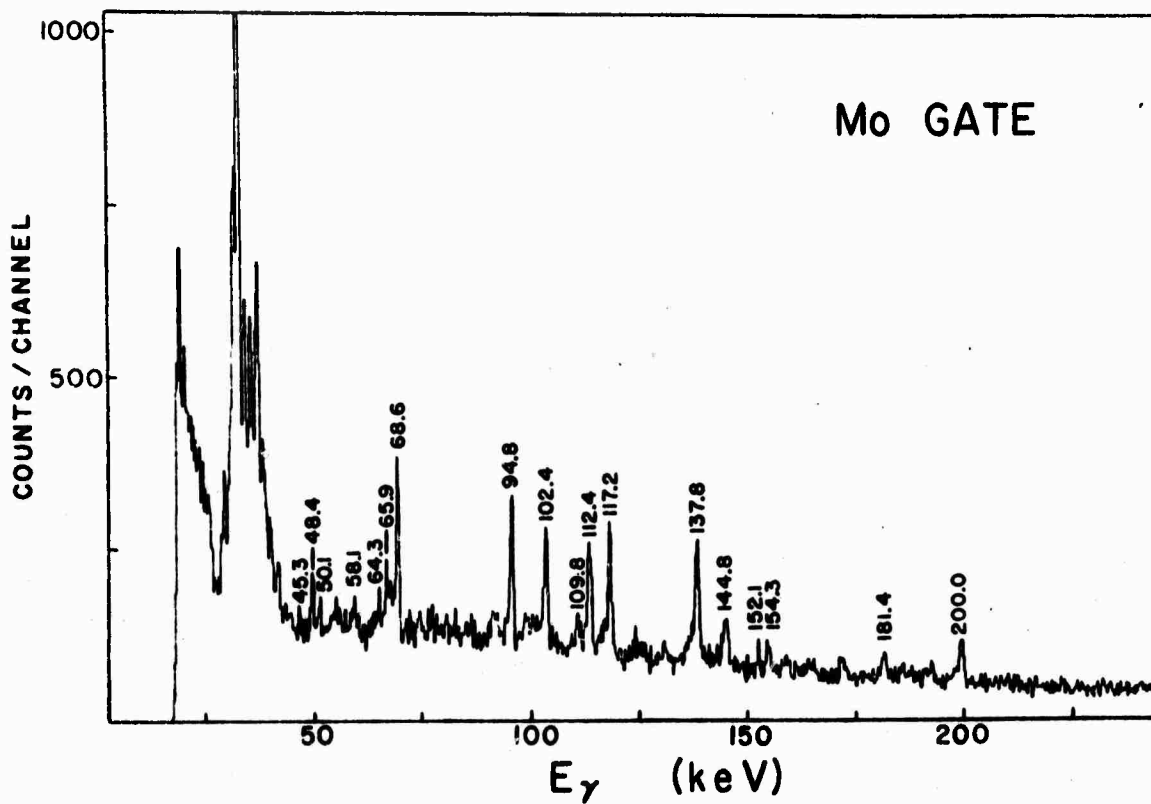


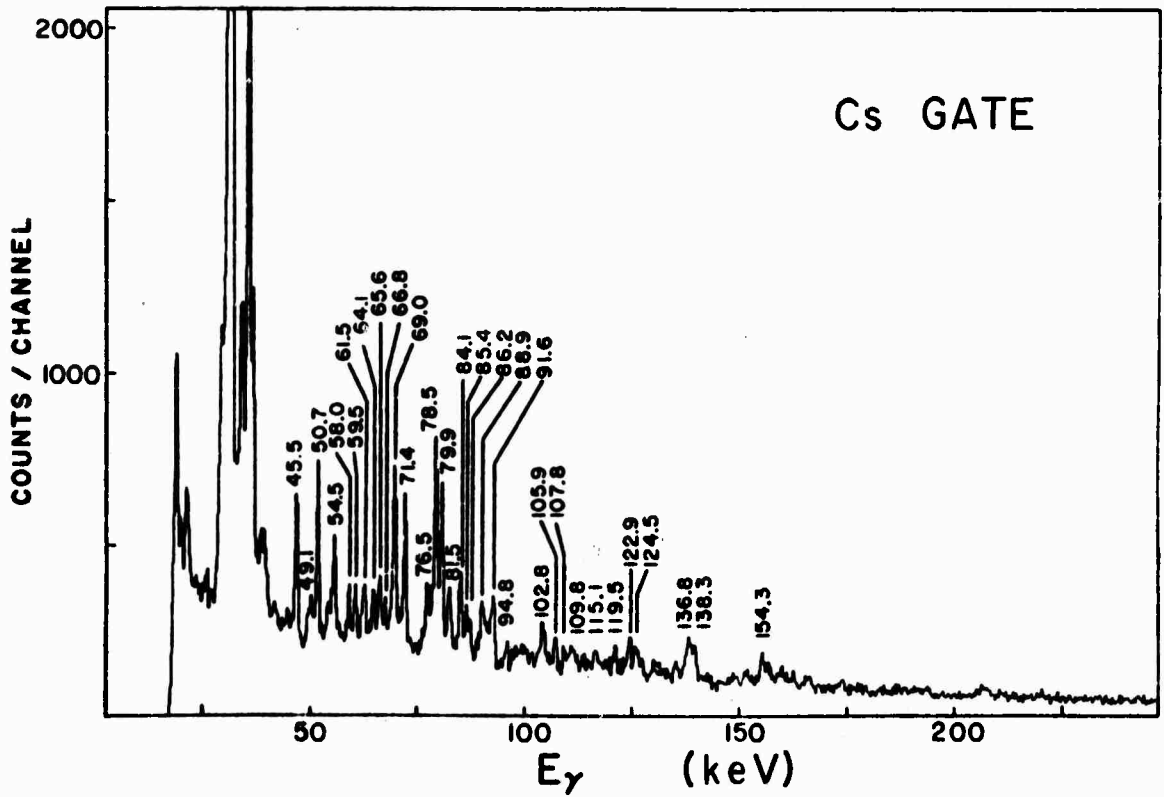
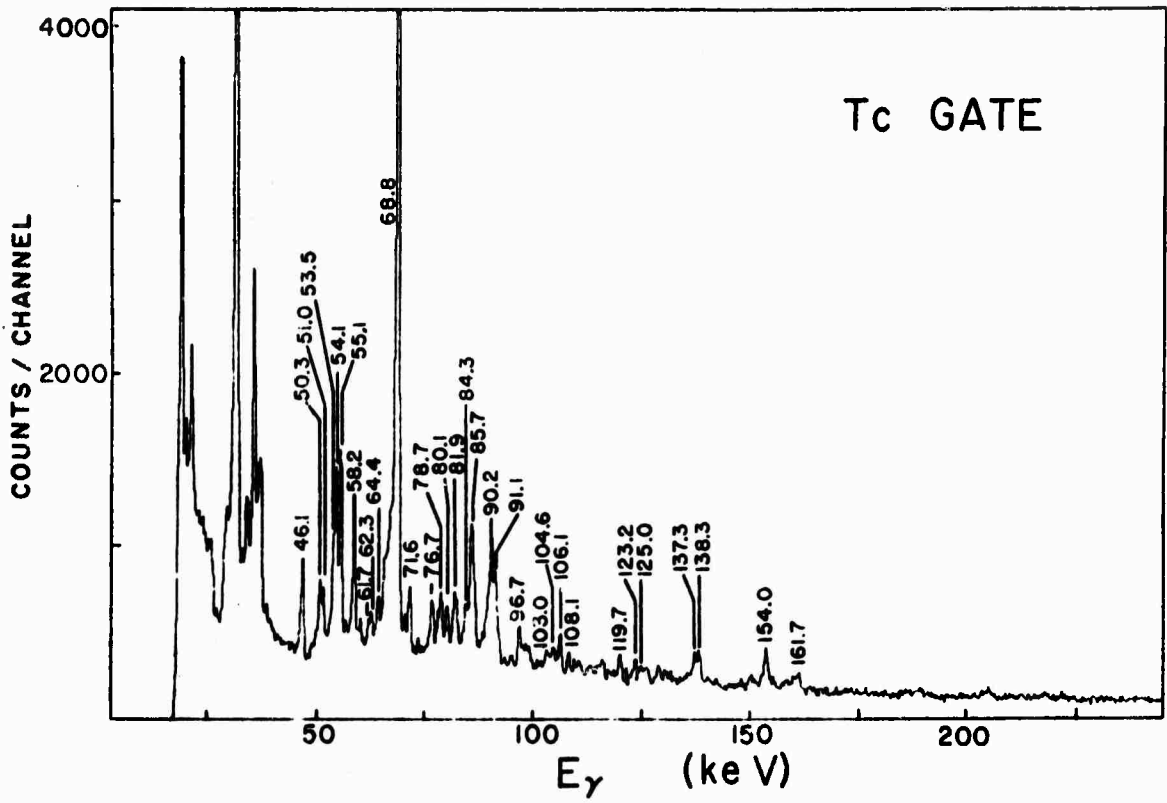




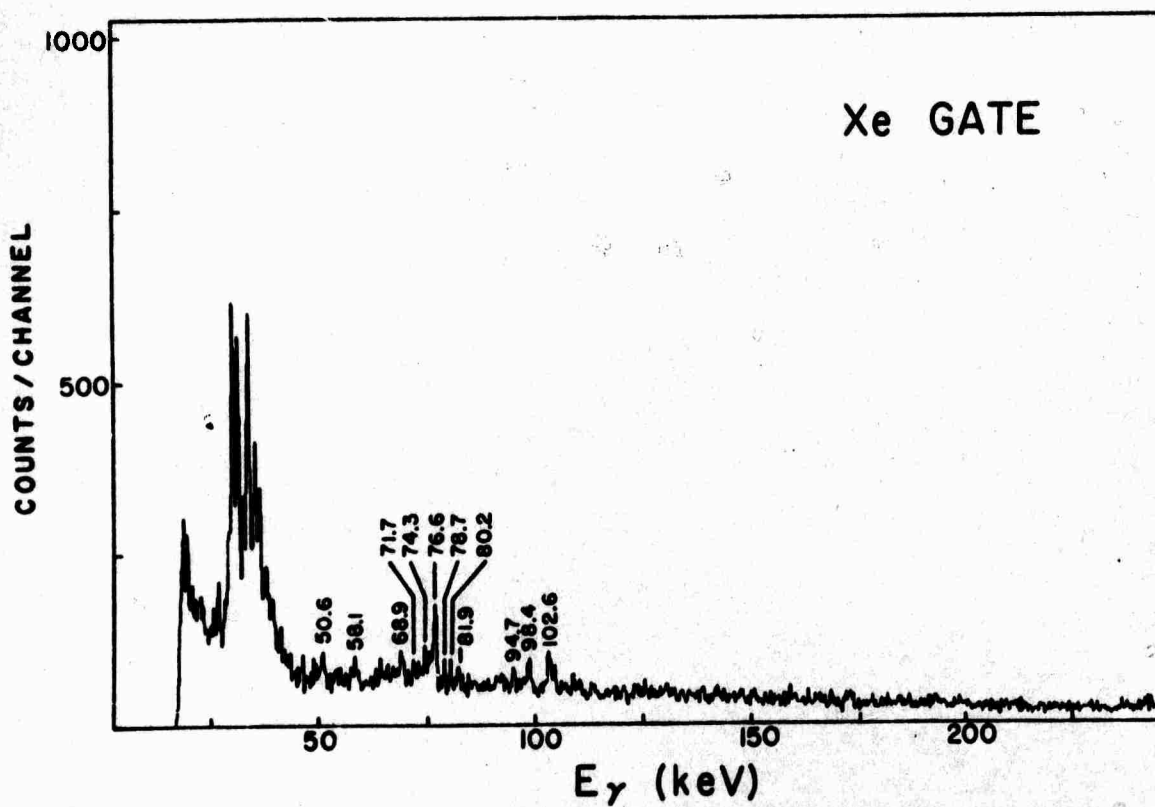
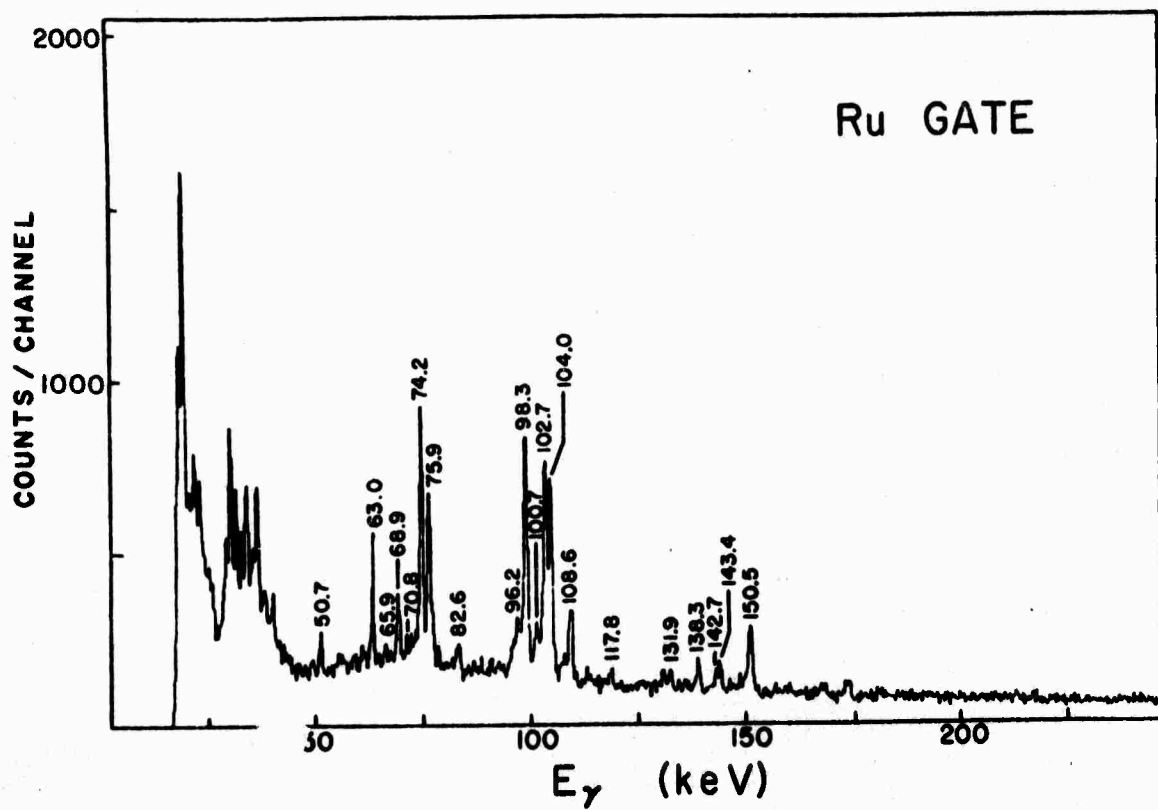


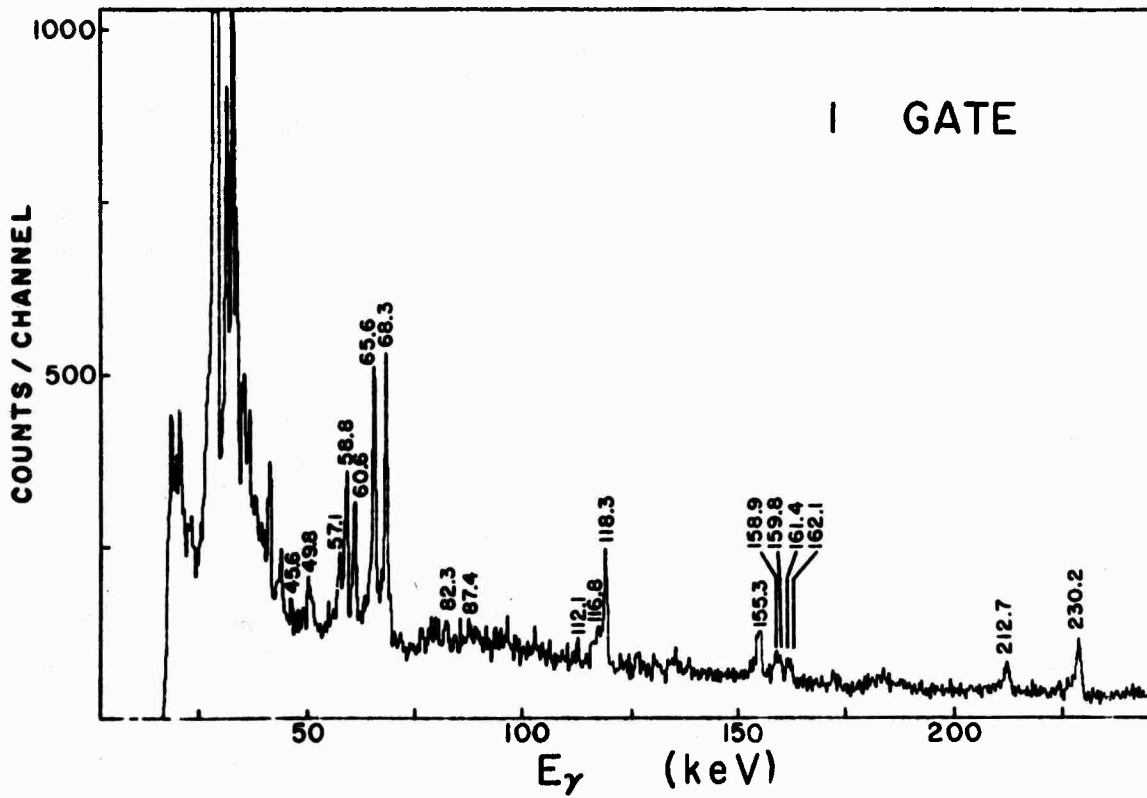
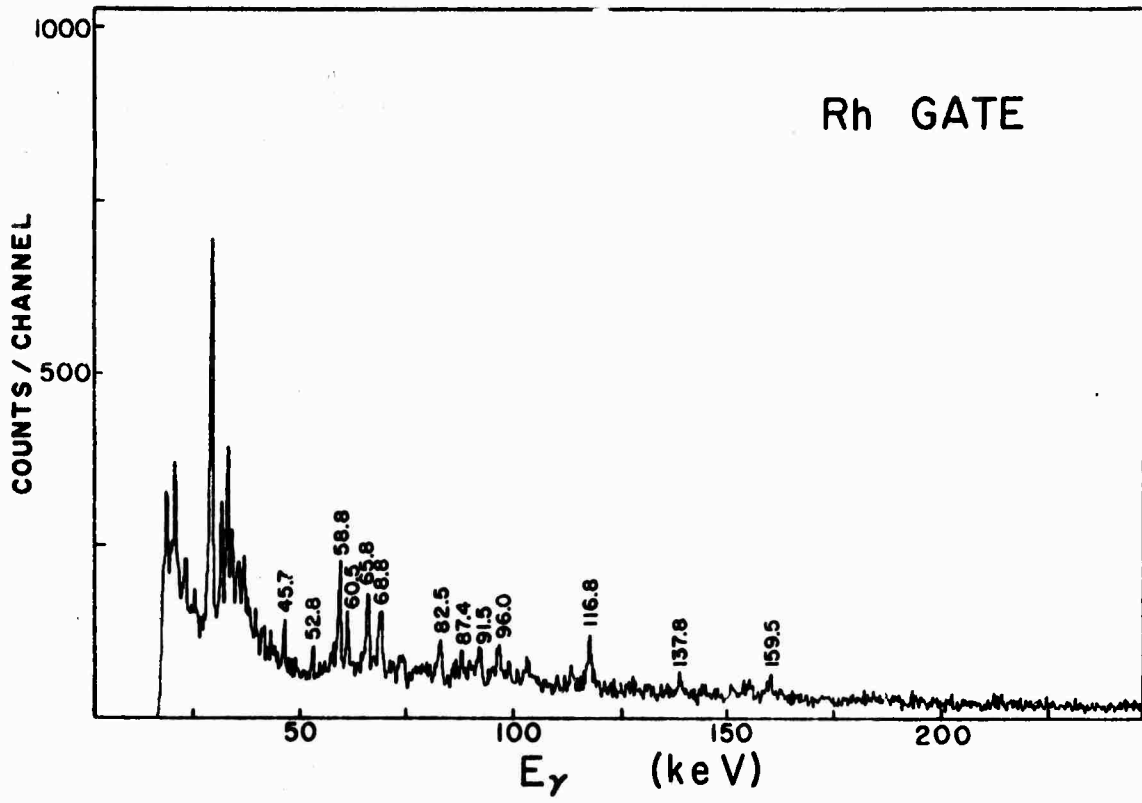


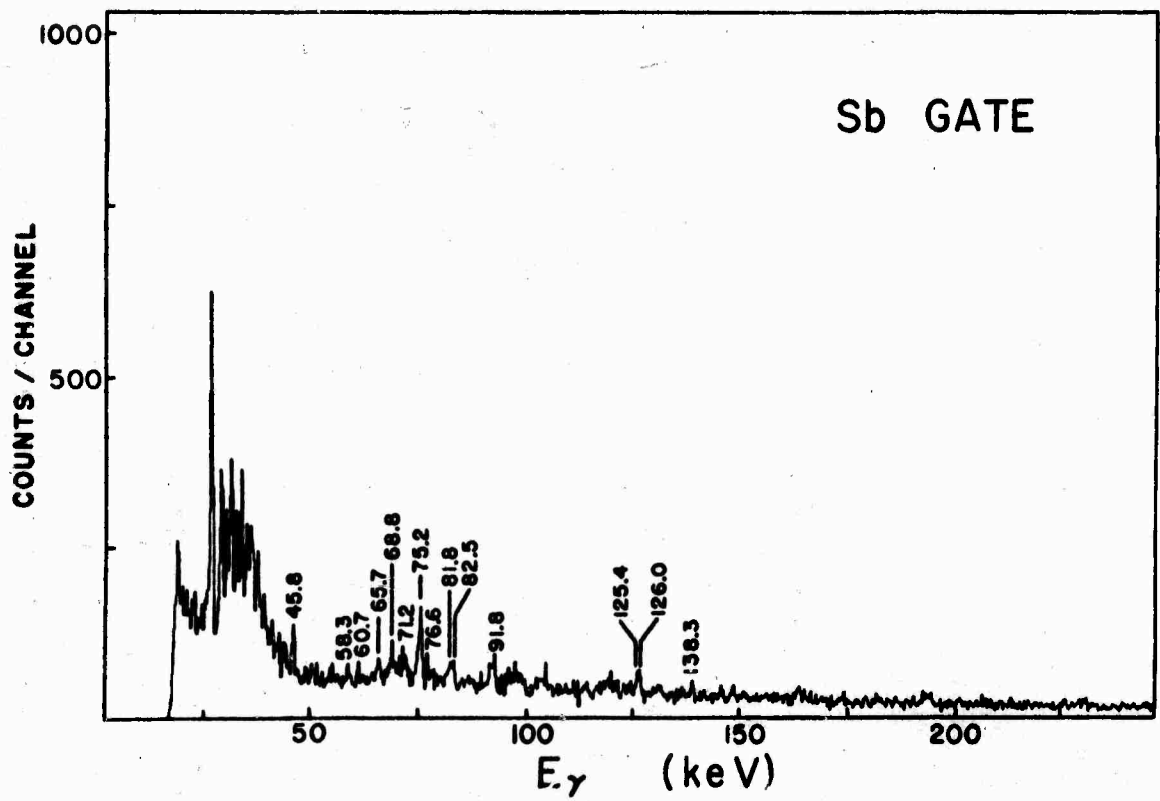
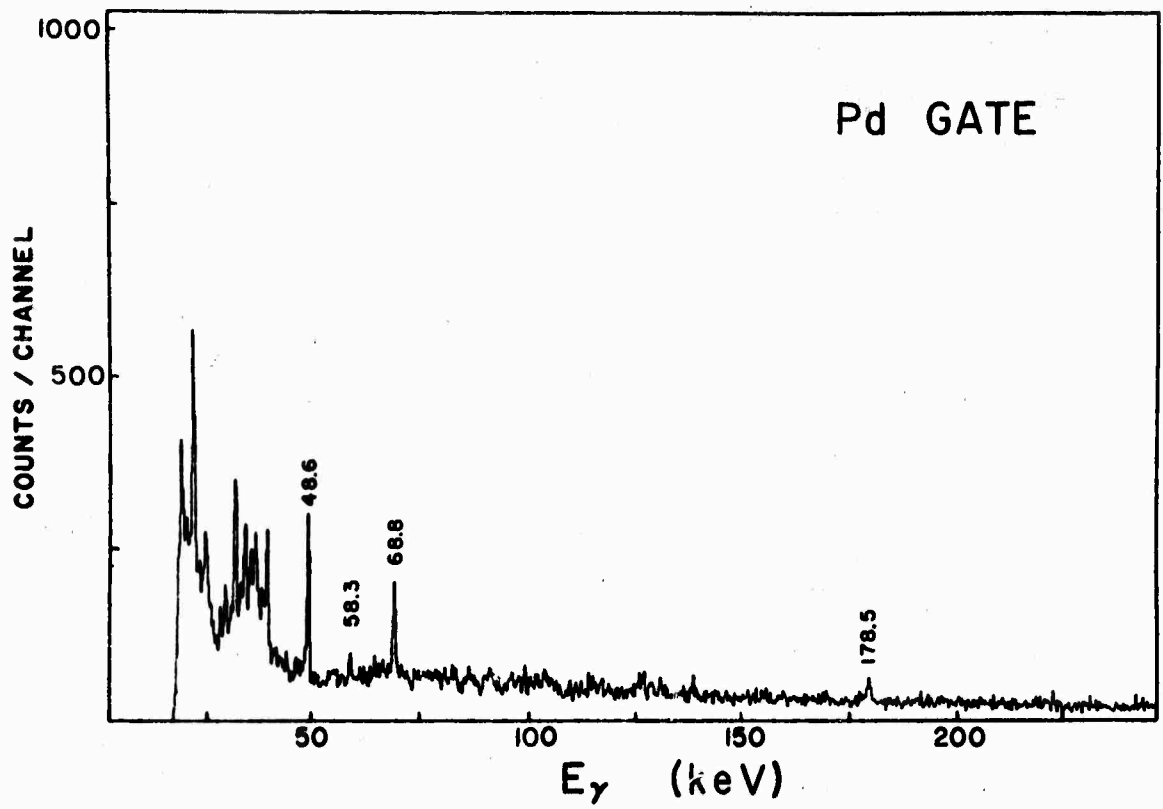




0.72







# GENERALIZED DECAY SCHEME (POST NEUTRON)

